

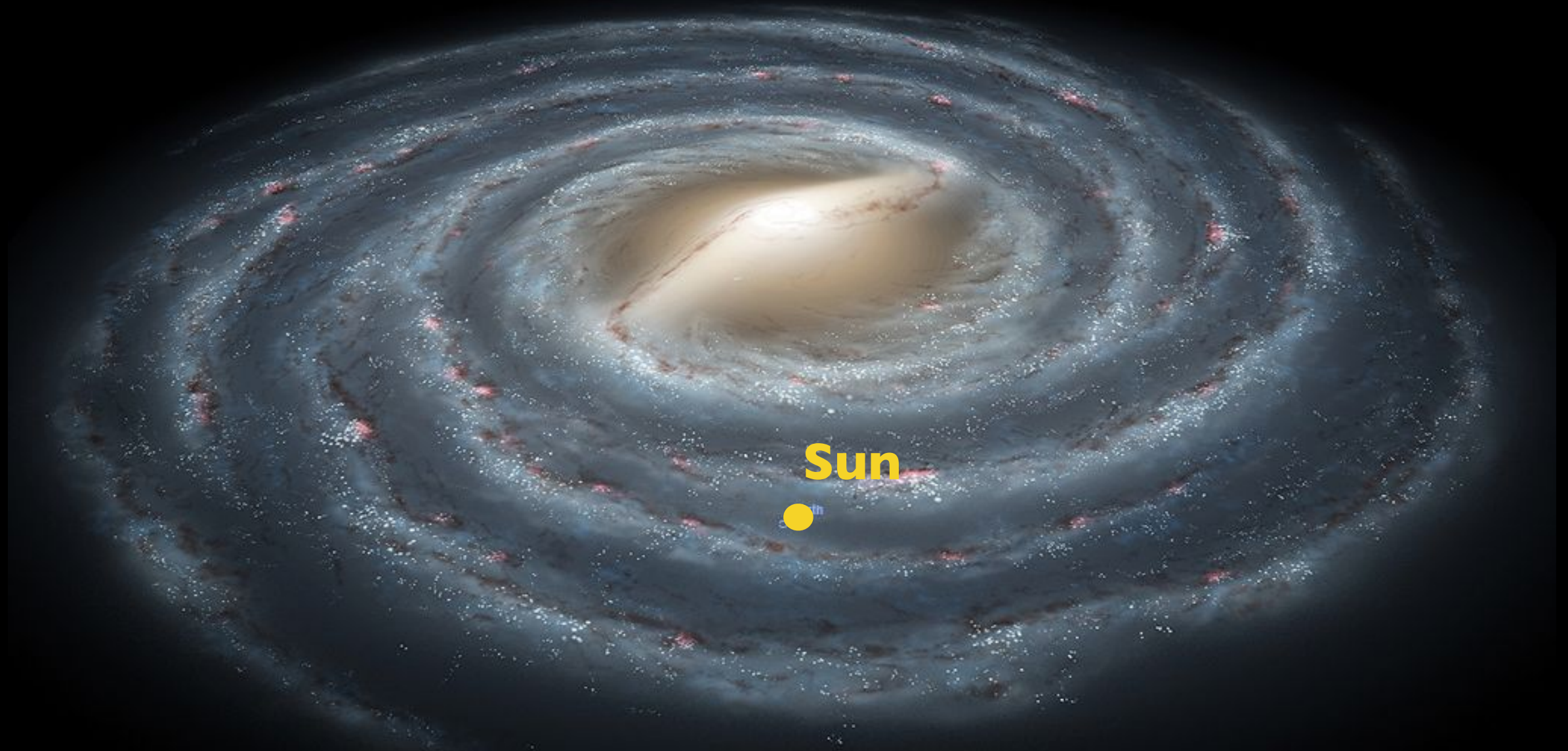
From cosmological simulations to dark matter direct detection

Nassim Bozorgnia

Institute for Particle Physics Phenomenology
Durham University

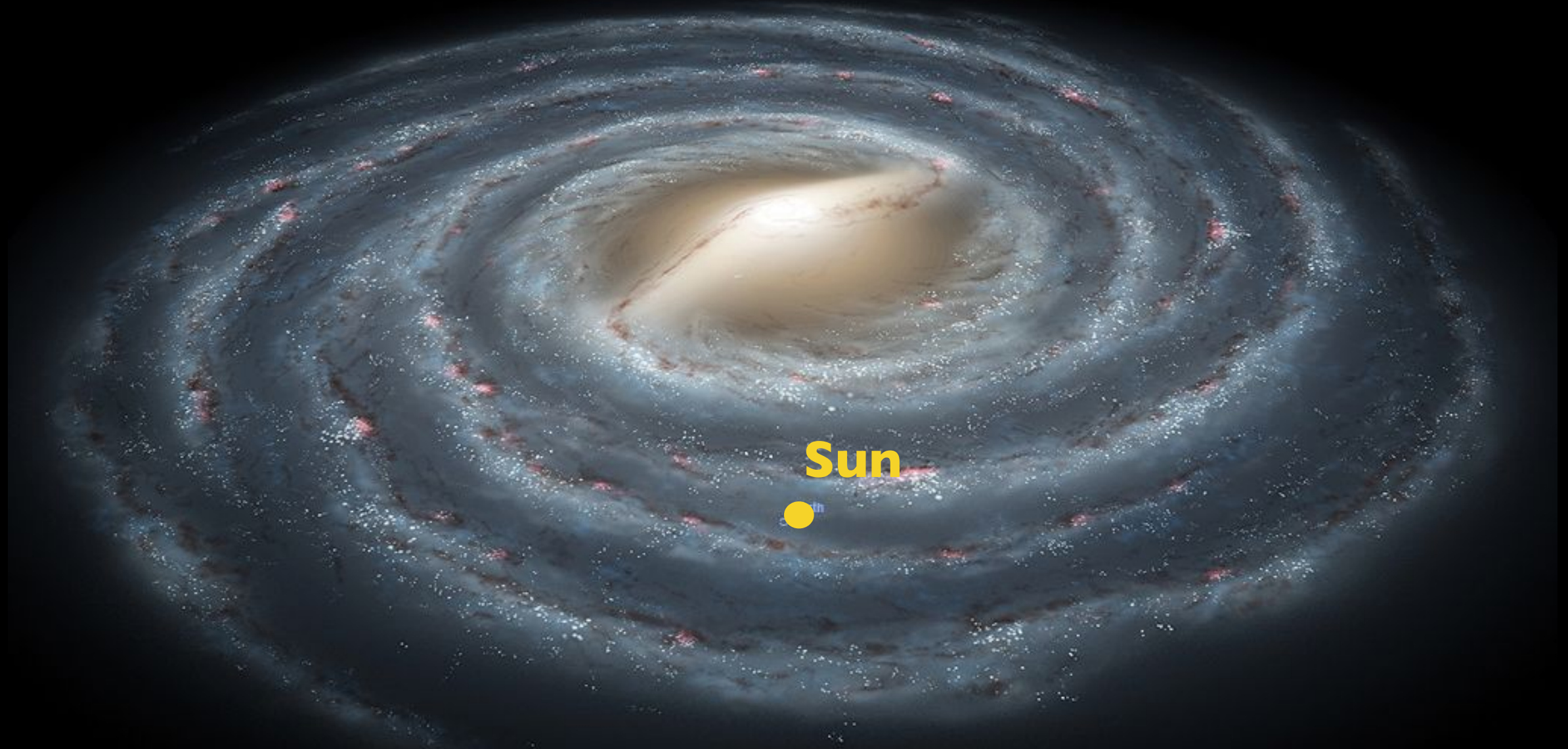
Local Dark Matter distribution

What is the dark matter (DM) distribution in the Solar neighborhood?



Local Dark Matter distribution

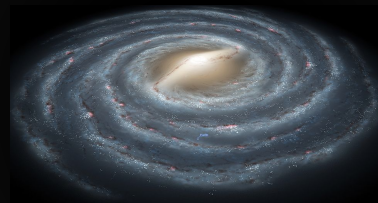
What is the dark matter (DM) distribution in the Solar neighborhood?



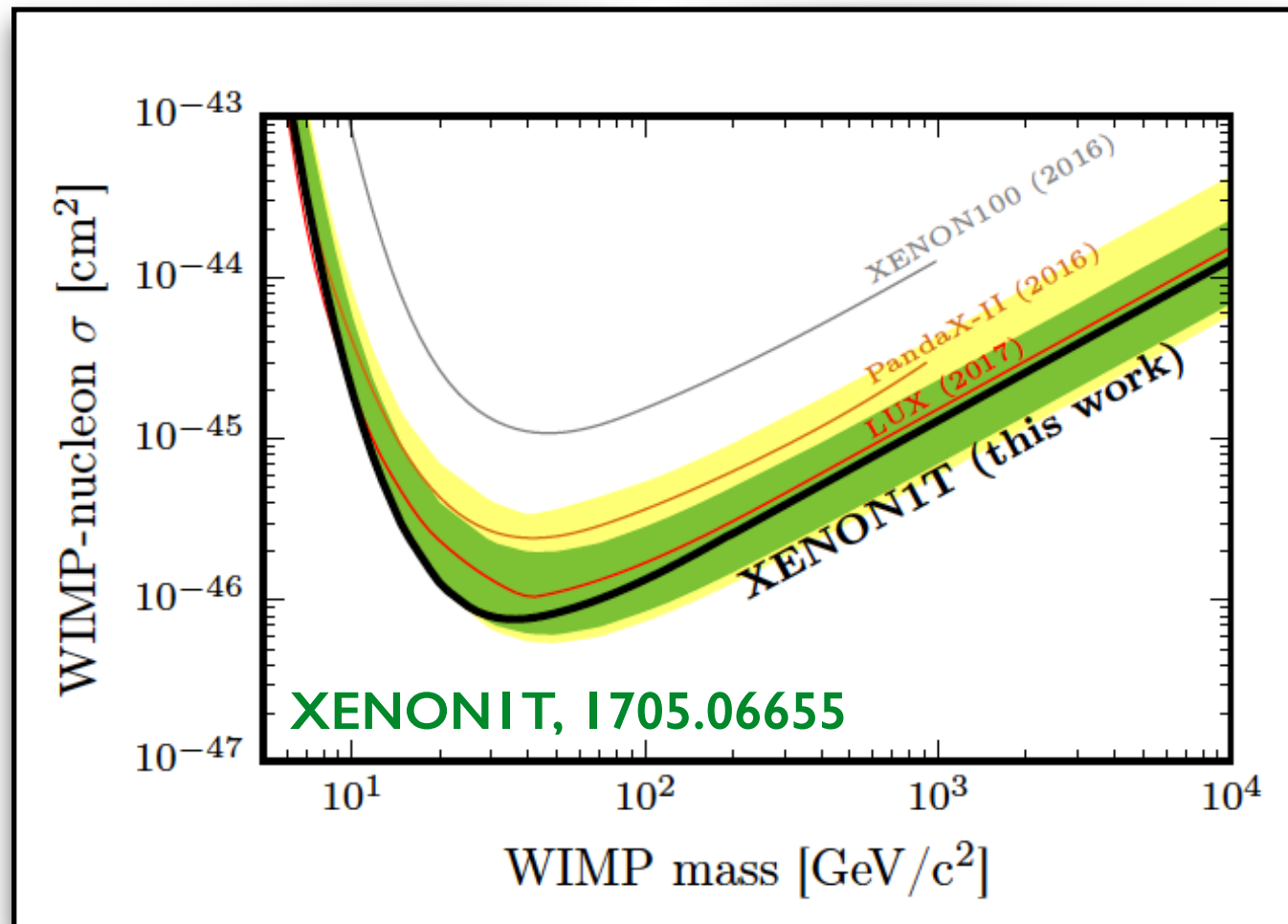
Uncertainties in the local DM distribution \longrightarrow **large uncertainties**
in the interpretation of direct detection data.

Dark Matter halo

- **Standard Halo model (SHM)**: isothermal sphere with an isotropic Maxwell-Boltzmann velocity distribution with a *peak speed* equal to the *local circular speed* (~ 220 km/s).

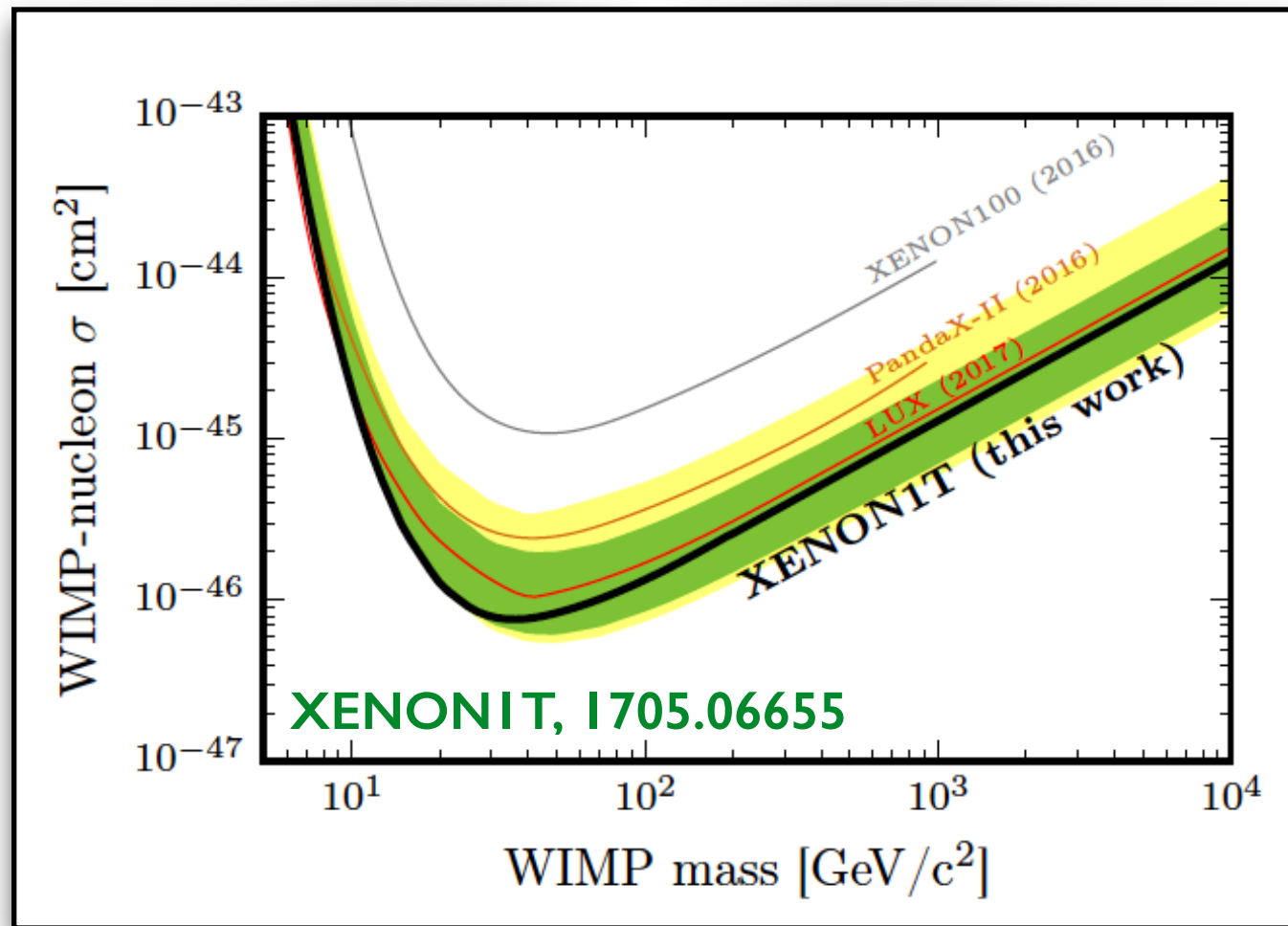


Astrophysical inputs



Assumption: **SHM**

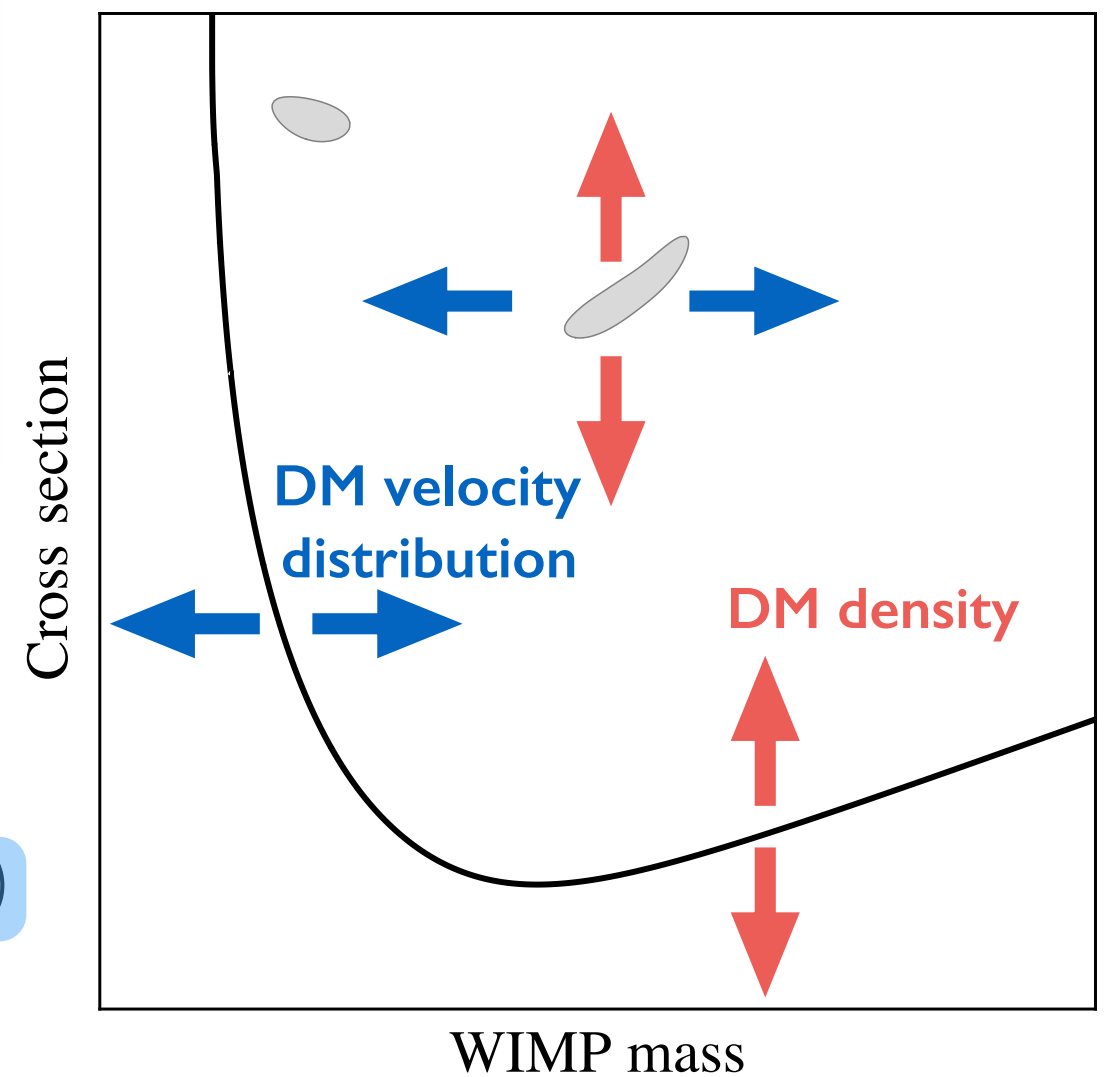
Astrophysical inputs



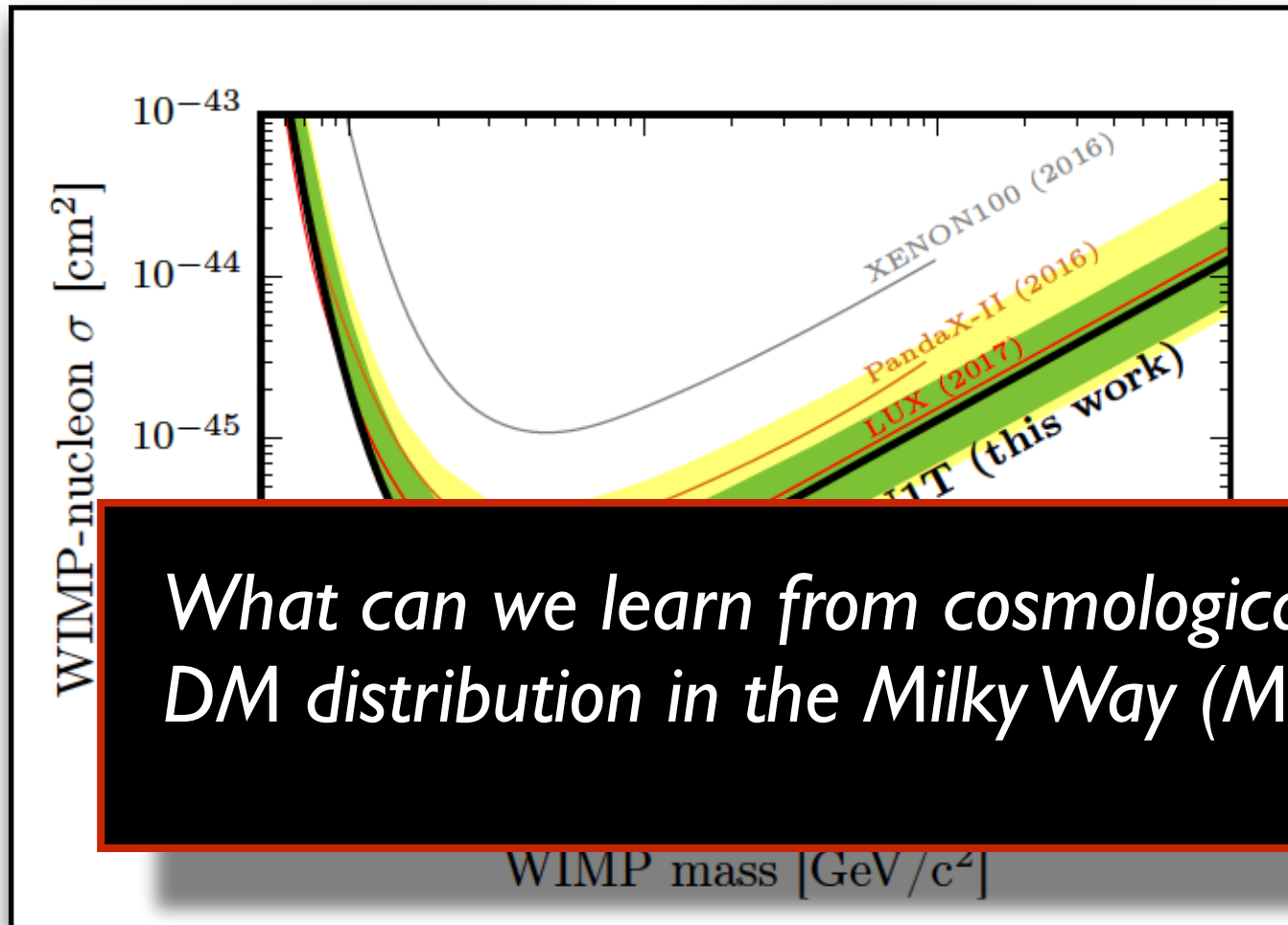
Assumption: **SHM**

$$\frac{dR}{dE_R} = \frac{\rho_\chi}{m_\chi m_N} \int_{v > v_{\min}} d^3v \frac{d\sigma_{\chi N}}{dE_R} v f_{\text{det}}(\mathbf{v}, t)$$

↖ astrophysics ↘



Astrophysical inputs

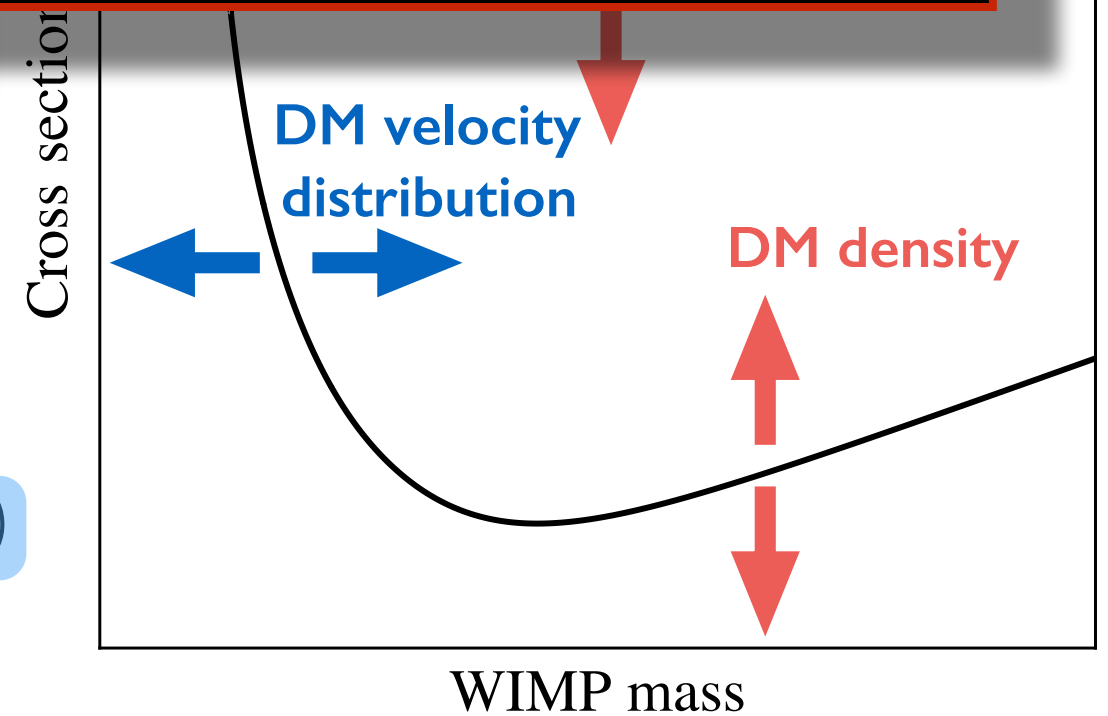


What can we learn from cosmological simulations about the local DM distribution in the Milky Way (MW)?

Assumption: **SHM**

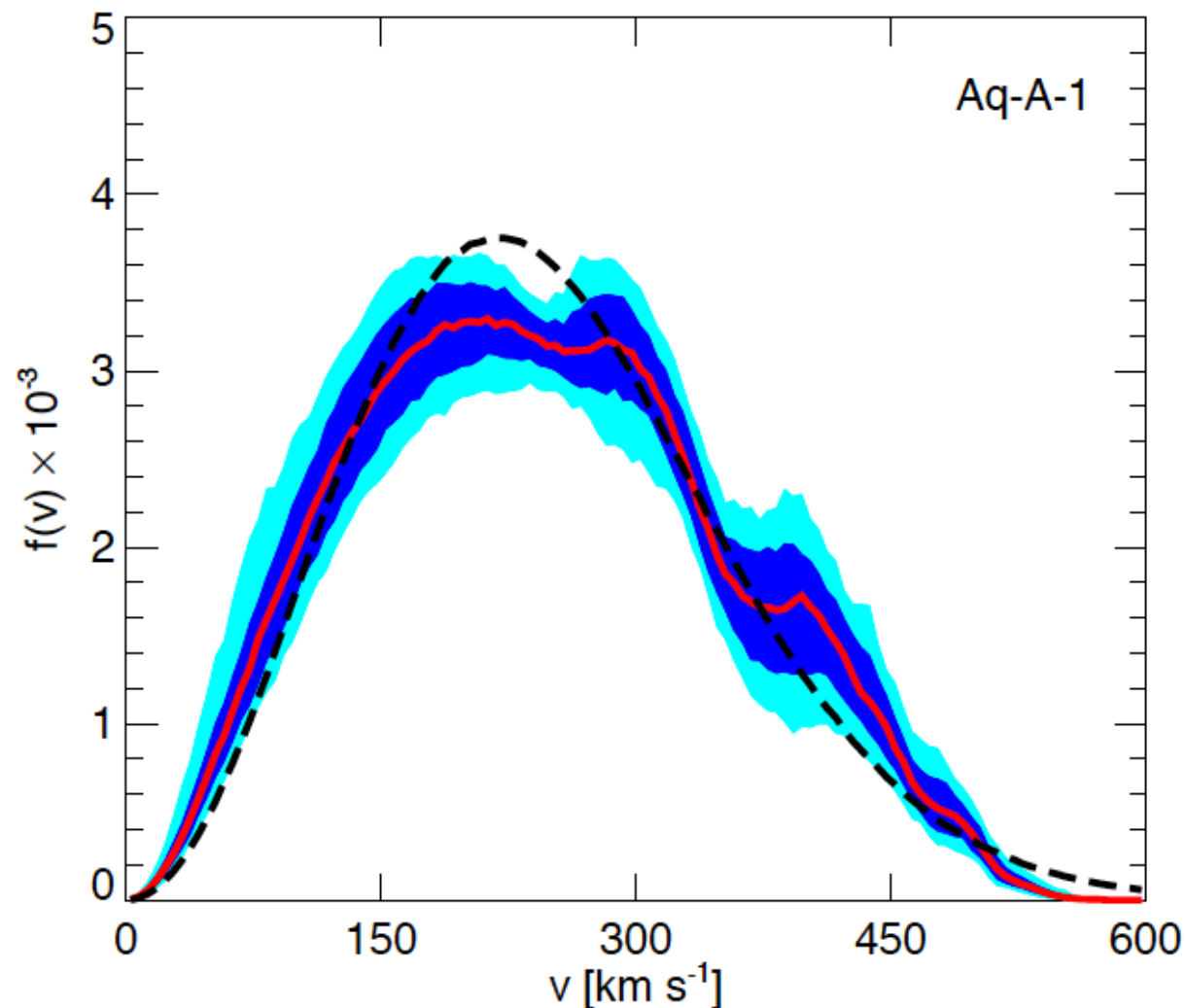
astrophysics

$$\frac{dR}{dE_R} = \frac{\rho_\chi}{m_\chi m_N} \int_{v > v_{\min}} d^3v \frac{d\sigma_{\chi N}}{dE_R} v f_{\text{det}}(\mathbf{v}, t)$$



Dark Matter only simulations

- DM speed distributions from cosmological N-body simulations **without baryons**, deviate substantially from a Maxwellian.



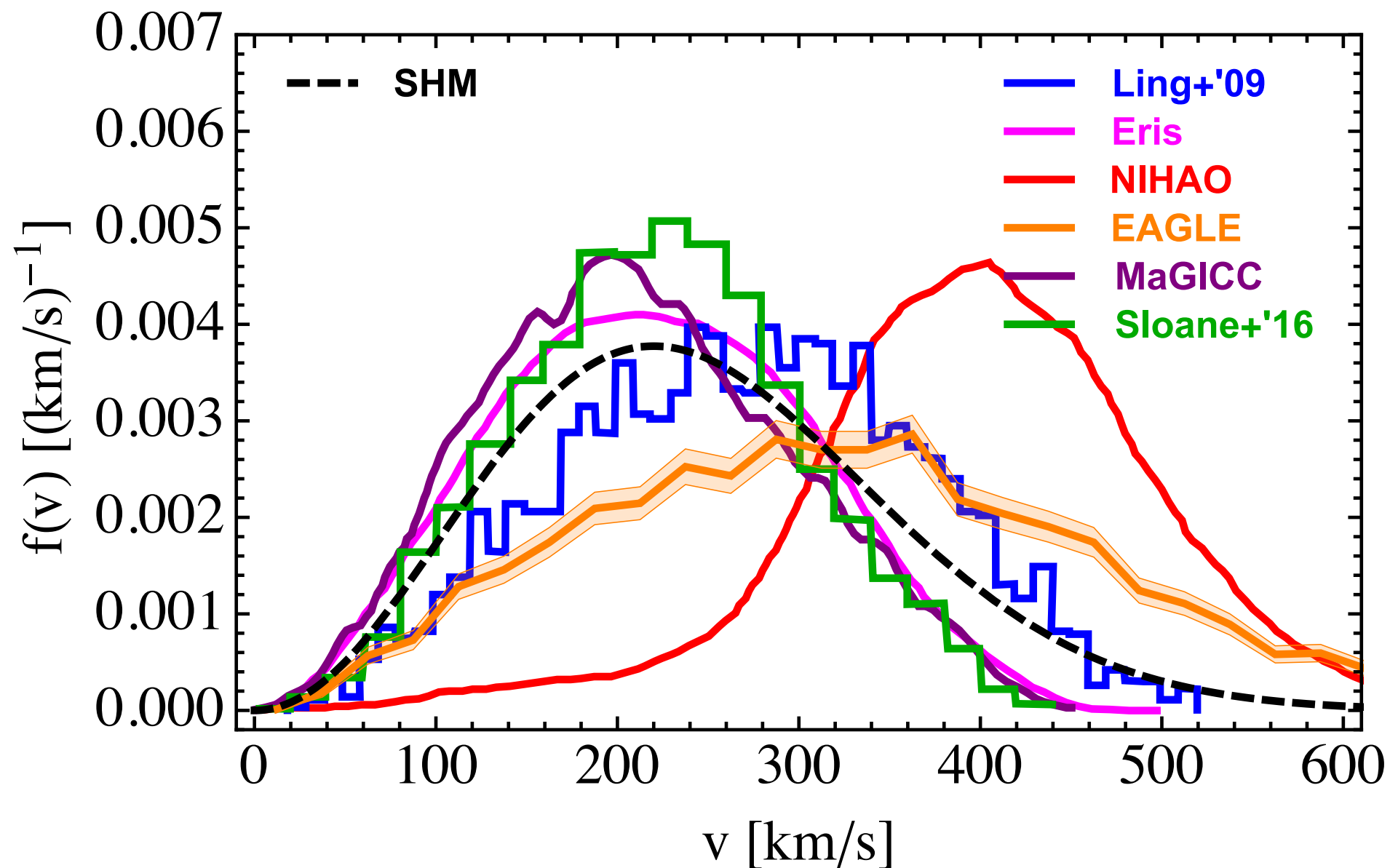
$$f(|\mathbf{v}|) = v^2 \int d\Omega_{\mathbf{v}} f(\mathbf{v})$$

Vogelsberger et al., 0812.0362

- Significant systematic uncertainty since the impact of baryons neglected.*

Hydrodynamical simulations

- Each hydrodynamical (**DM + baryons**) simulation adopts a different *galaxy formation model, spatial resolution, DM particle mass*.

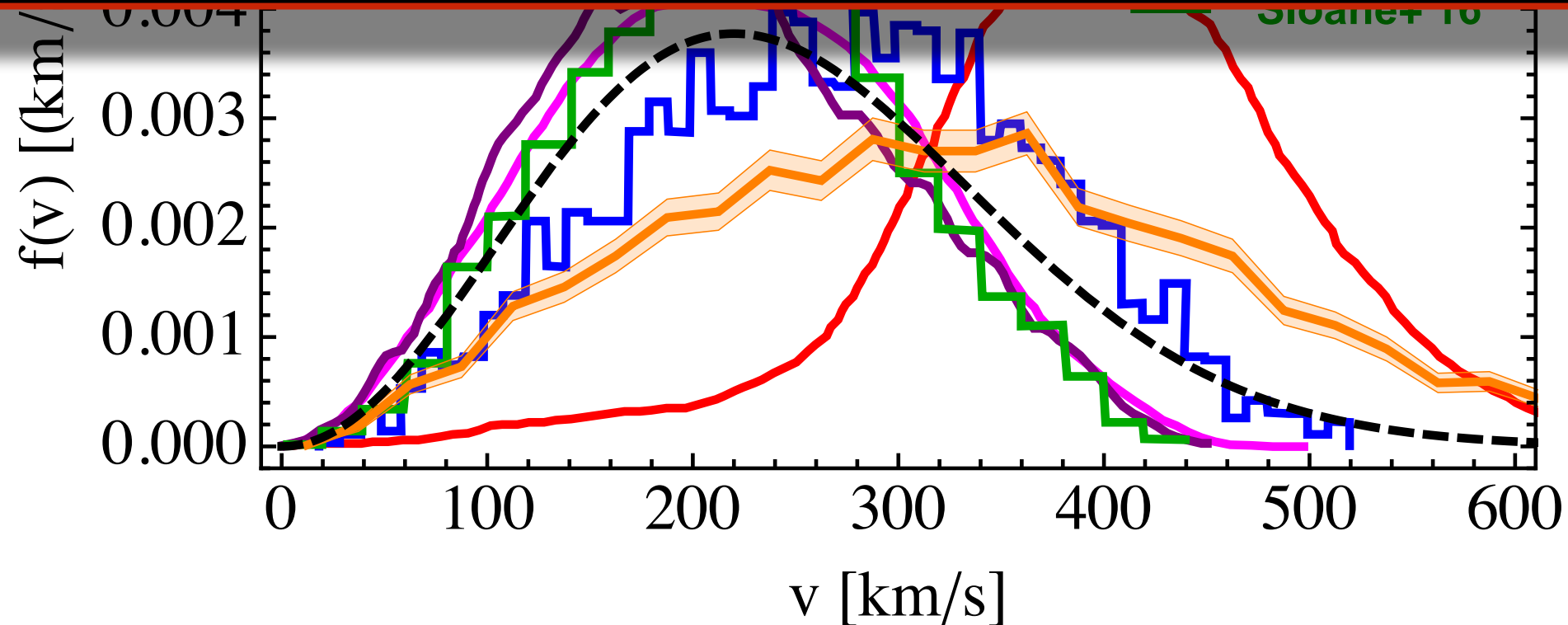


Bozorgnia & Bertone, 1705.05853

Hydrodynamical simulations

- Each hydrodynamical (**DM + baryons**) simulation adopts a different *galaxy formation model, spatial resolution, DM particle mass*.

Different criteria used to identify MW-like galaxies among different groups. The most common criterion is the MW mass constraint, which has a large uncertainty.

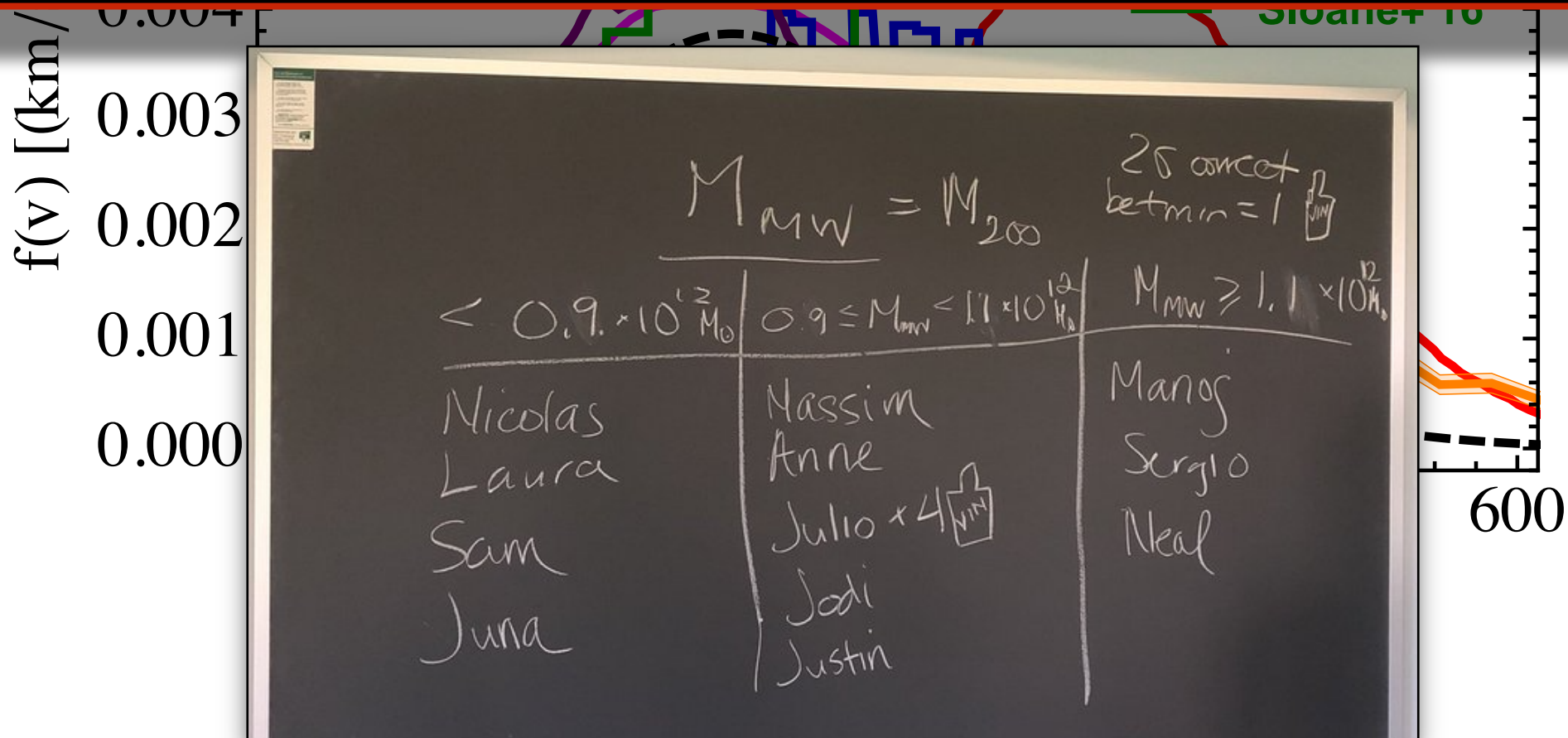


Bozorgnia & Bertone, 1705.05853

Hydrodynamical simulations

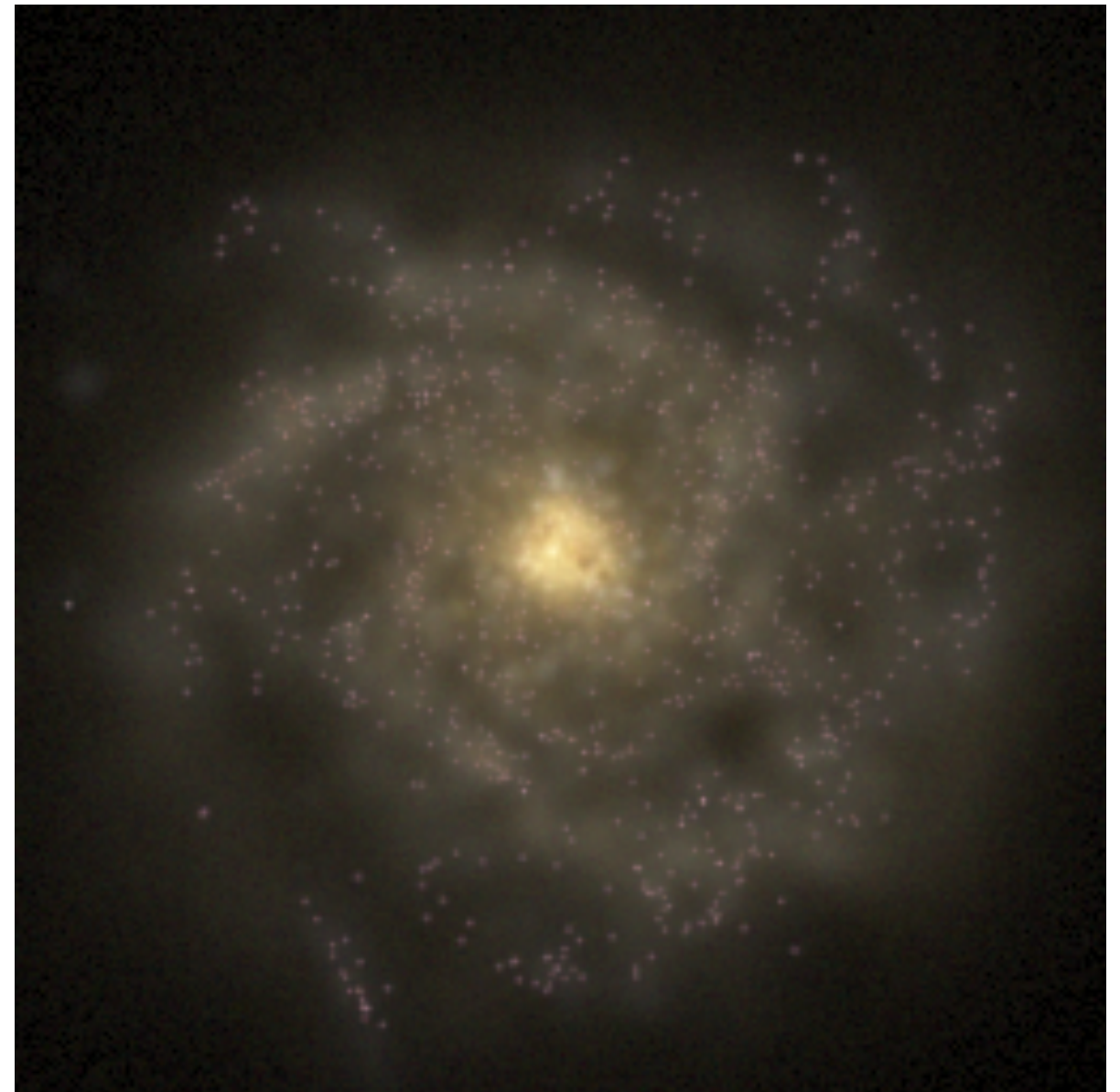
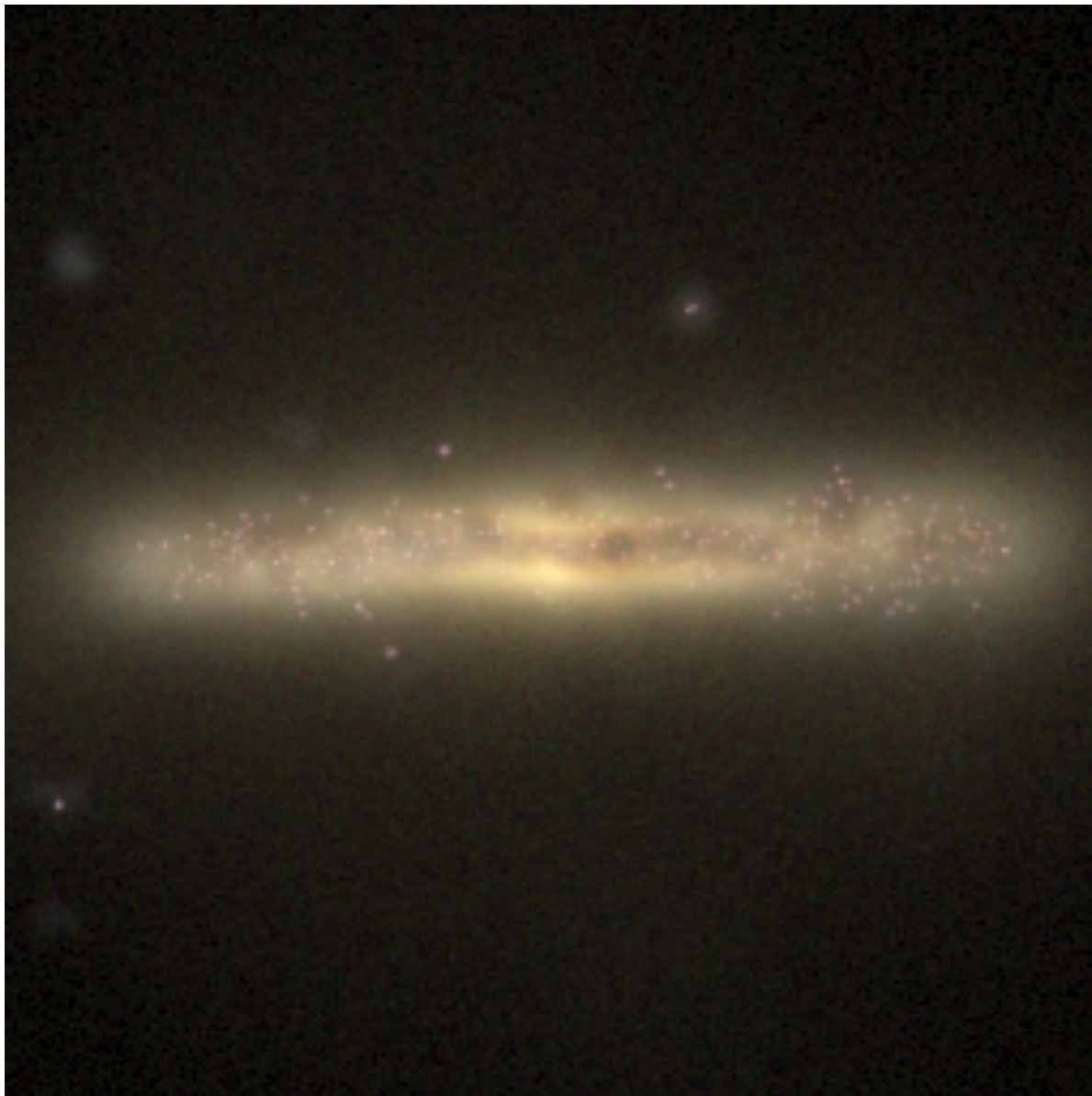
- Each hydrodynamical (**DM + baryons**) simulation adopts a different *galaxy formation model, spatial resolution, DM particle mass*.

Different criteria used to identify MW-like galaxies among different groups. The most common criterion is the MW mass constraint, which has a large uncertainty.



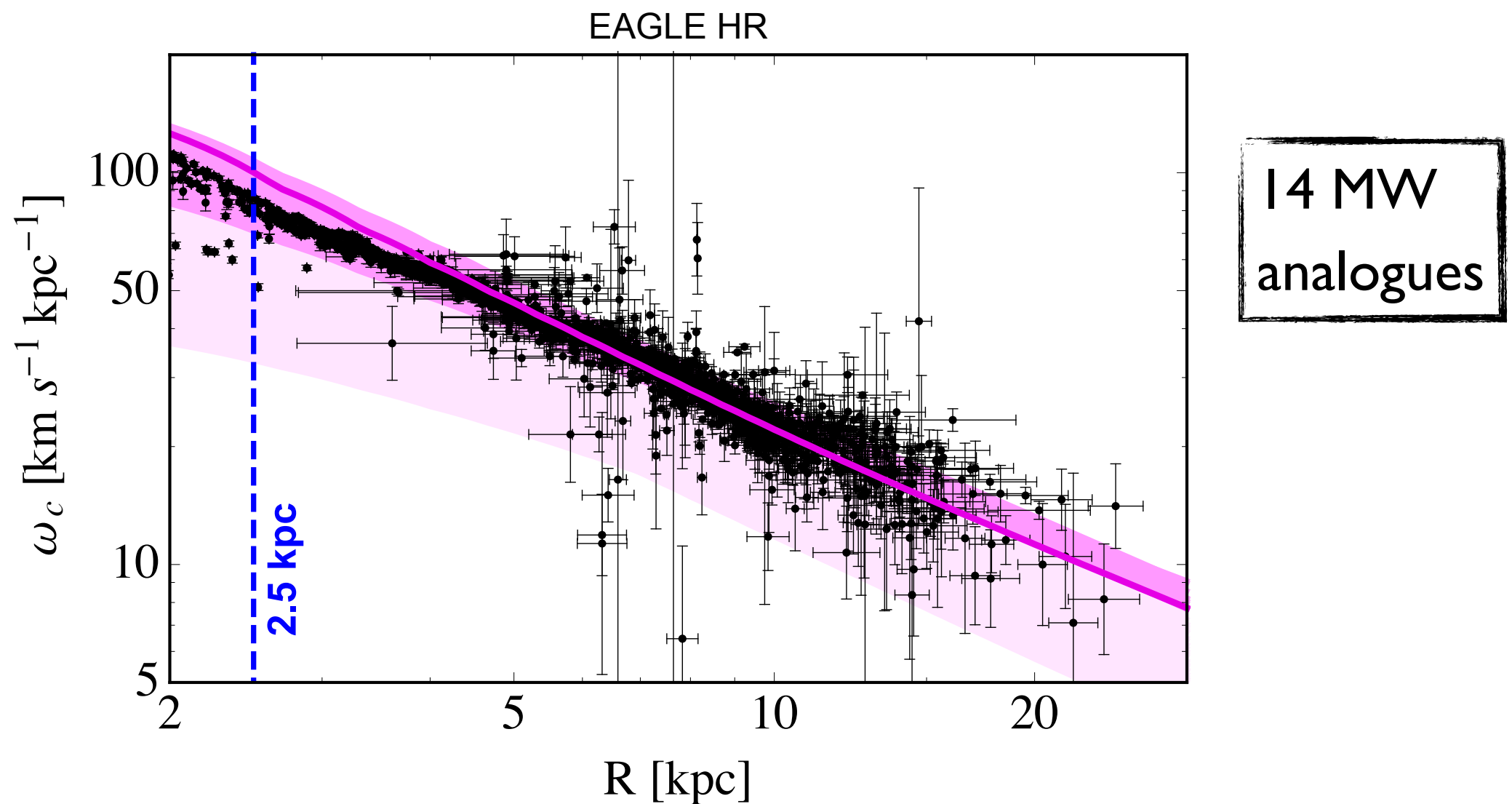
EAGLE and APOSTLE

- We use the **EAGLE** and **APOSTLE** hydrodynamic simulations. *Calibrated to reproduce the observed distribution of stellar masses and sizes of low-redshift galaxies.*



Identifying Milky Way analogues

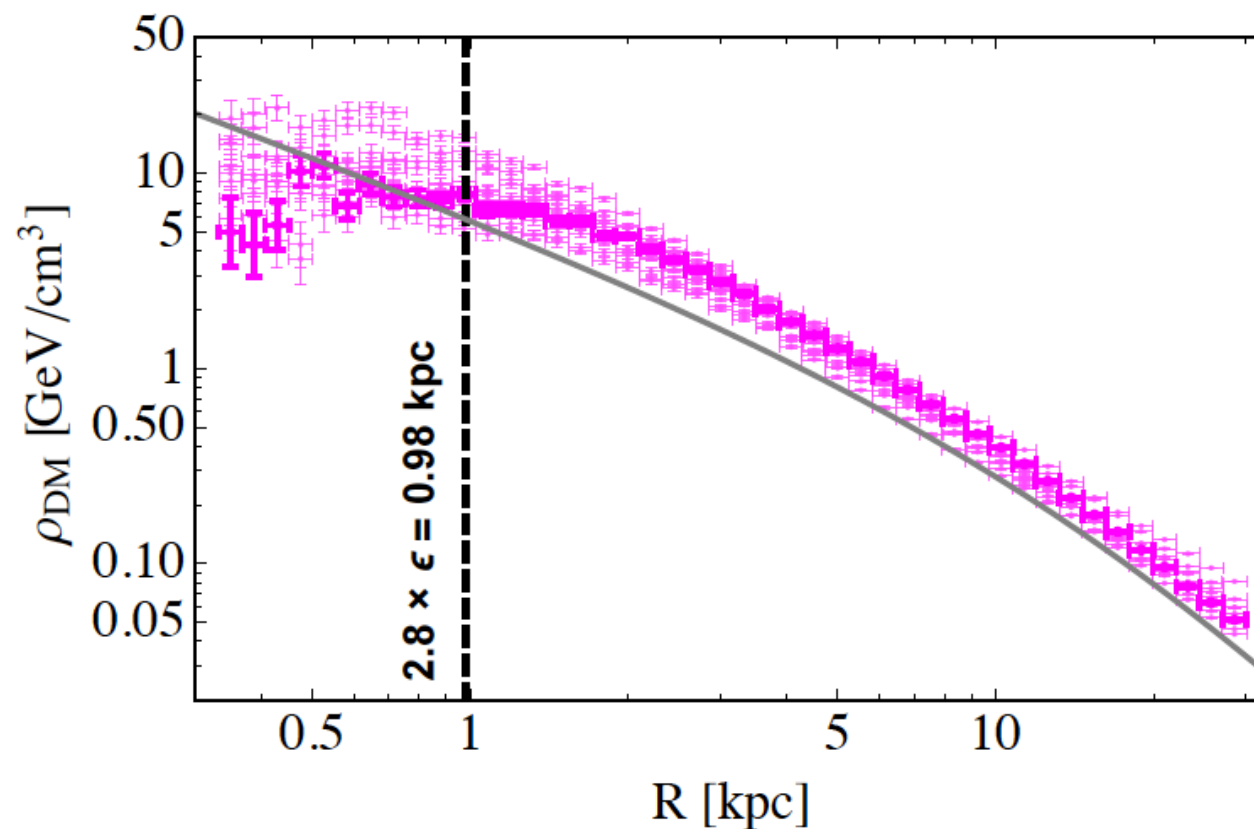
- Identify MW-like galaxies by taking into account observational constraints on the MW, in addition to the mass constraint:
rotation curves [Iocco, Pato, Bertone, 1502.03821], **total stellar mass**.



Bozorgnia et al., 1601.04707
Calore, Bozorgnia et al., 1509.02164

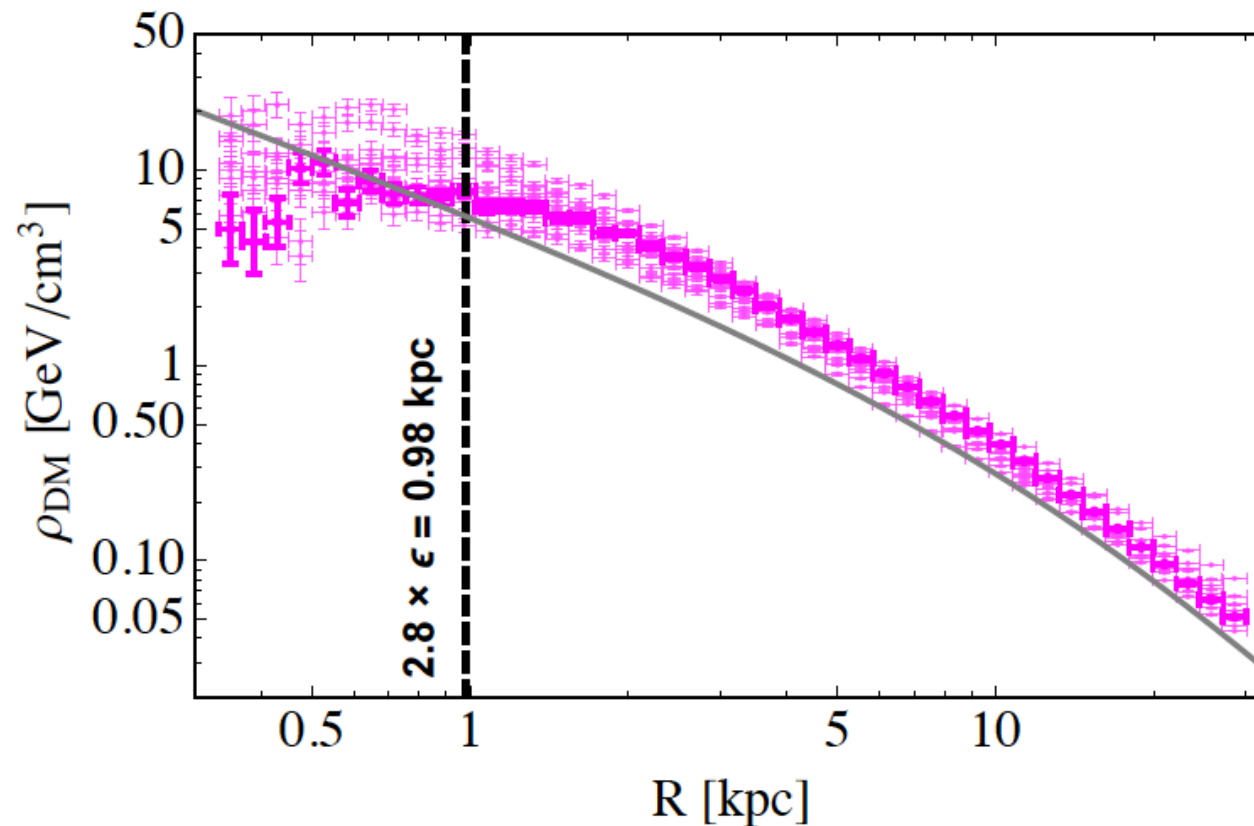
Dark Matter density profiles

- Spherically averaged DM density profiles of the MW analogues:



Dark Matter density profiles

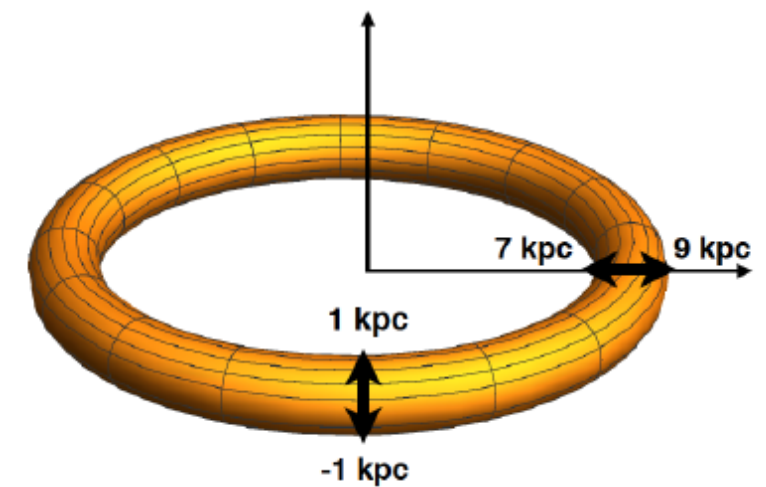
- Spherically averaged DM density profiles of the MW analogues:



- To find the DM density at the position of the Sun, consider a torus aligned with the stellar disc.

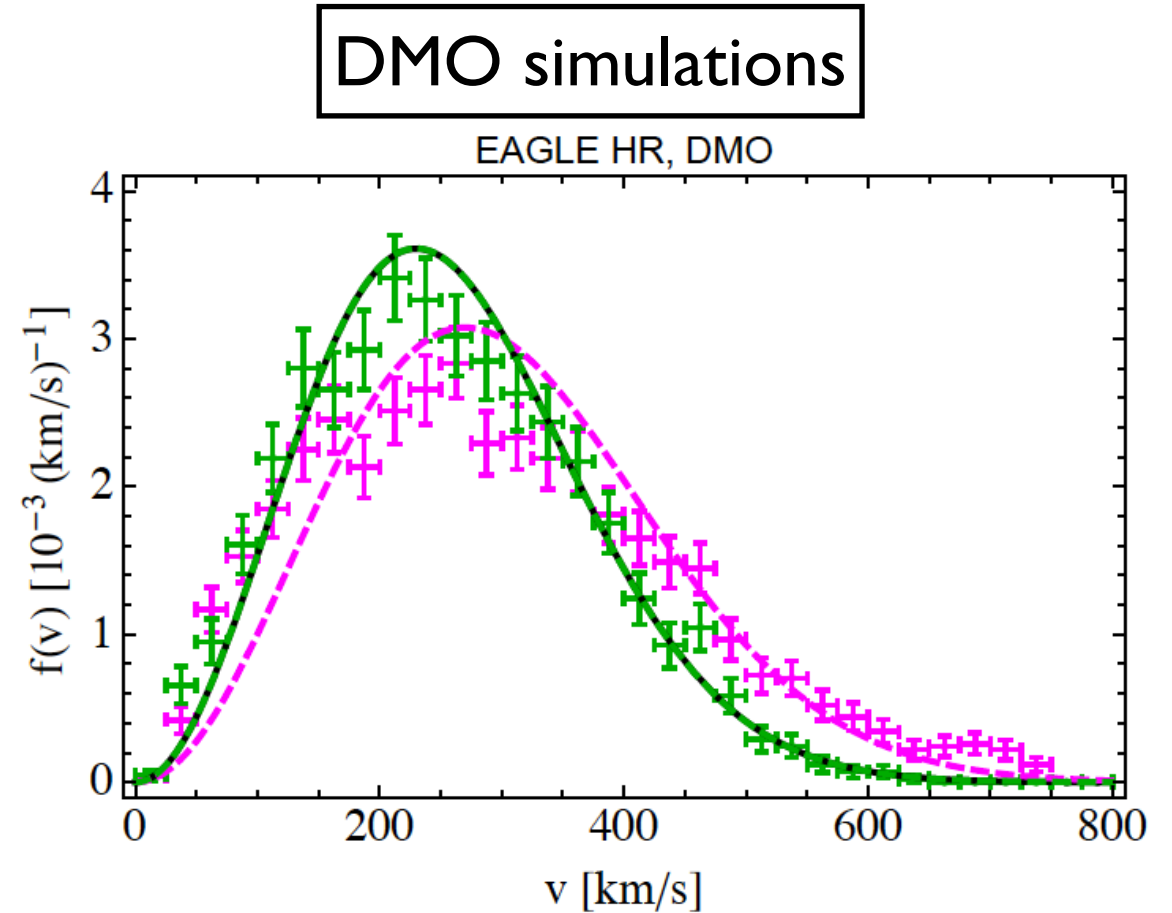
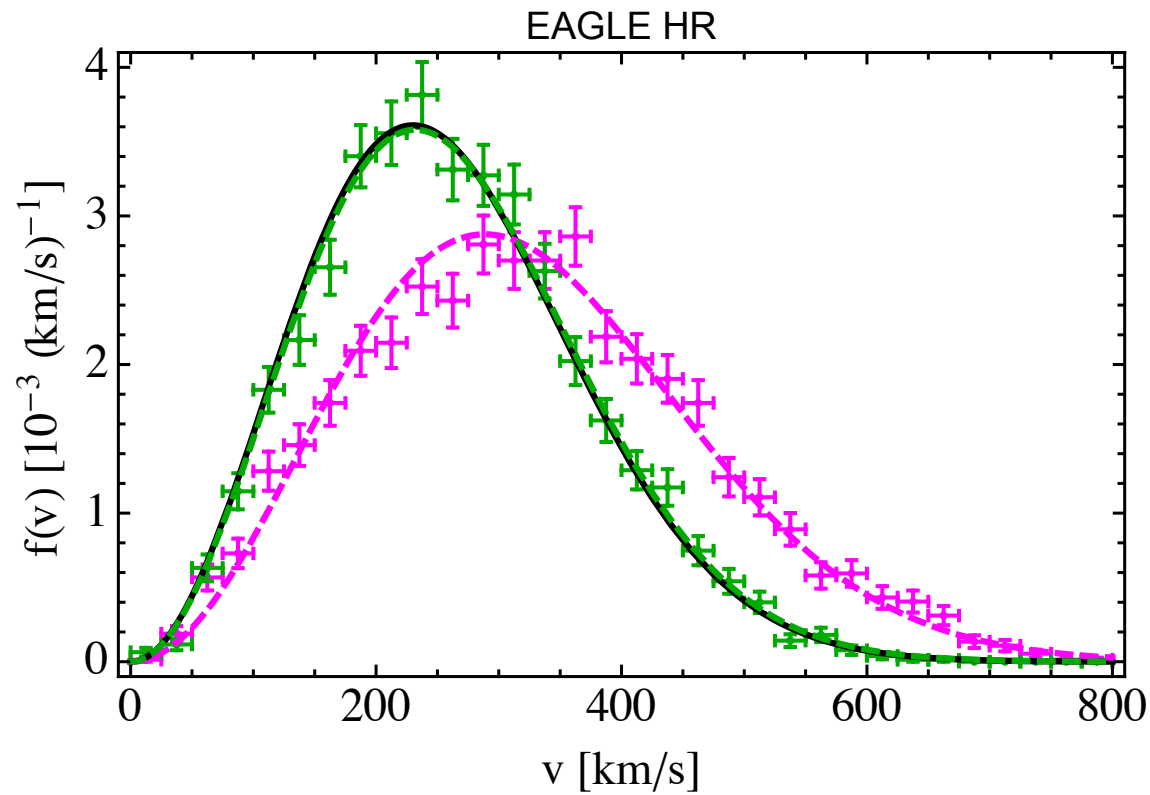
$$\rho_\chi = 0.41 - 0.73 \text{ GeV/cm}^3$$

Bozorgnia et al., 1601.04707



Local speed distributions

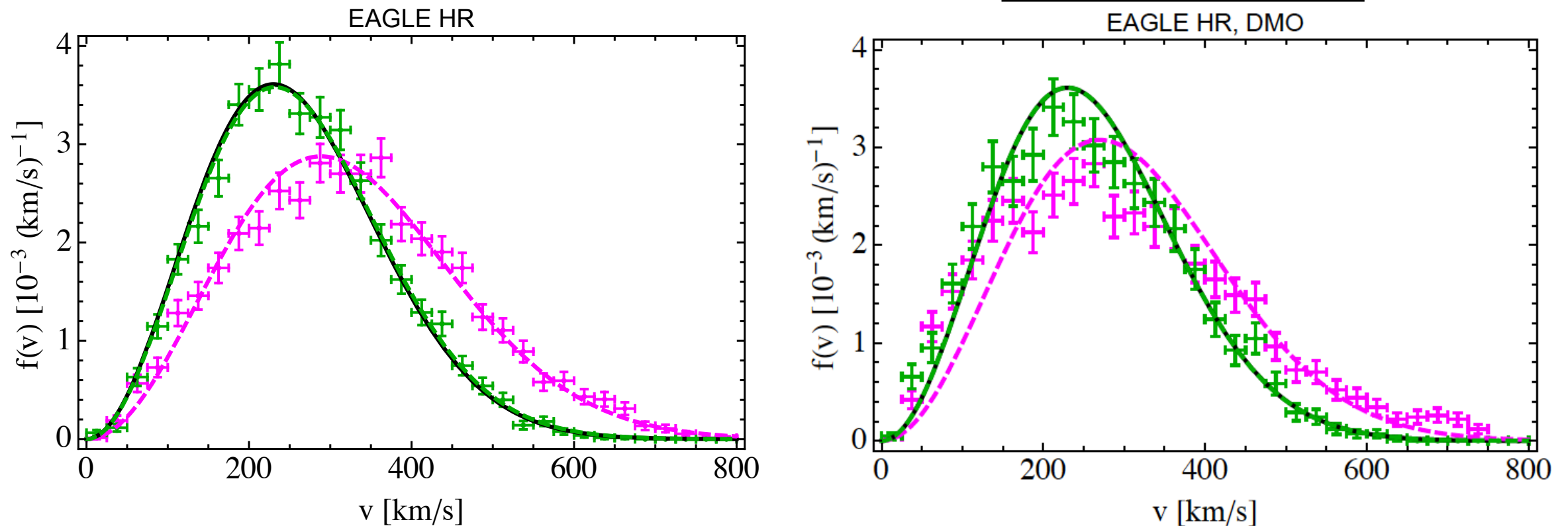
In the galactic rest frame:



Bozorgnia et al., 1601.04707

Local speed distributions

In the galactic rest frame:



Bozorgnia et al., 1601.04707

- Maxwellian distribution with a free peak provides a better fit to haloes in the hydrodynamical simulations compared to their DMO counterparts.
- Best fit peak speed: $v_{\text{peak}} = 223 - 289 \text{ km/s}$

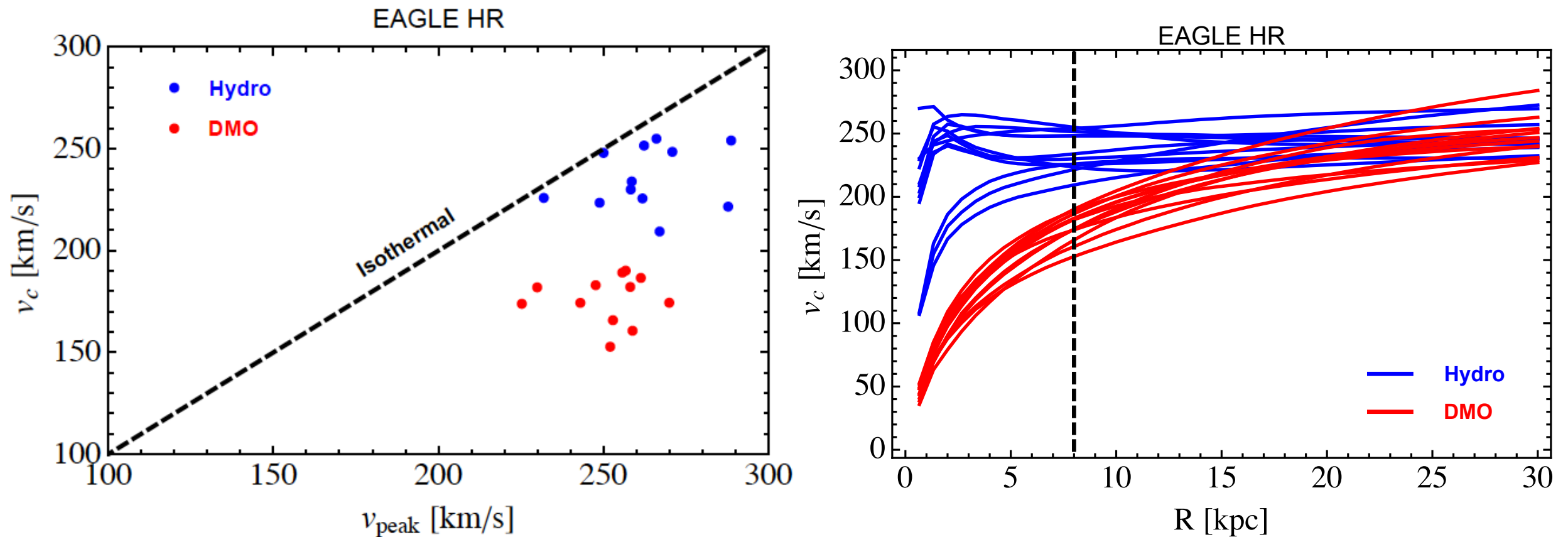
Local speed distributions

Common trends in different hydrodynamical simulations:

- Baryons deepen the gravitational potential in the inner halo, shifting the peak of the DM speed distribution to *higher speeds*.
- In most cases, baryons appear to make the local DM speed distribution *more Maxwellian*.

Bozorgnia & Bertone, 1705.05853

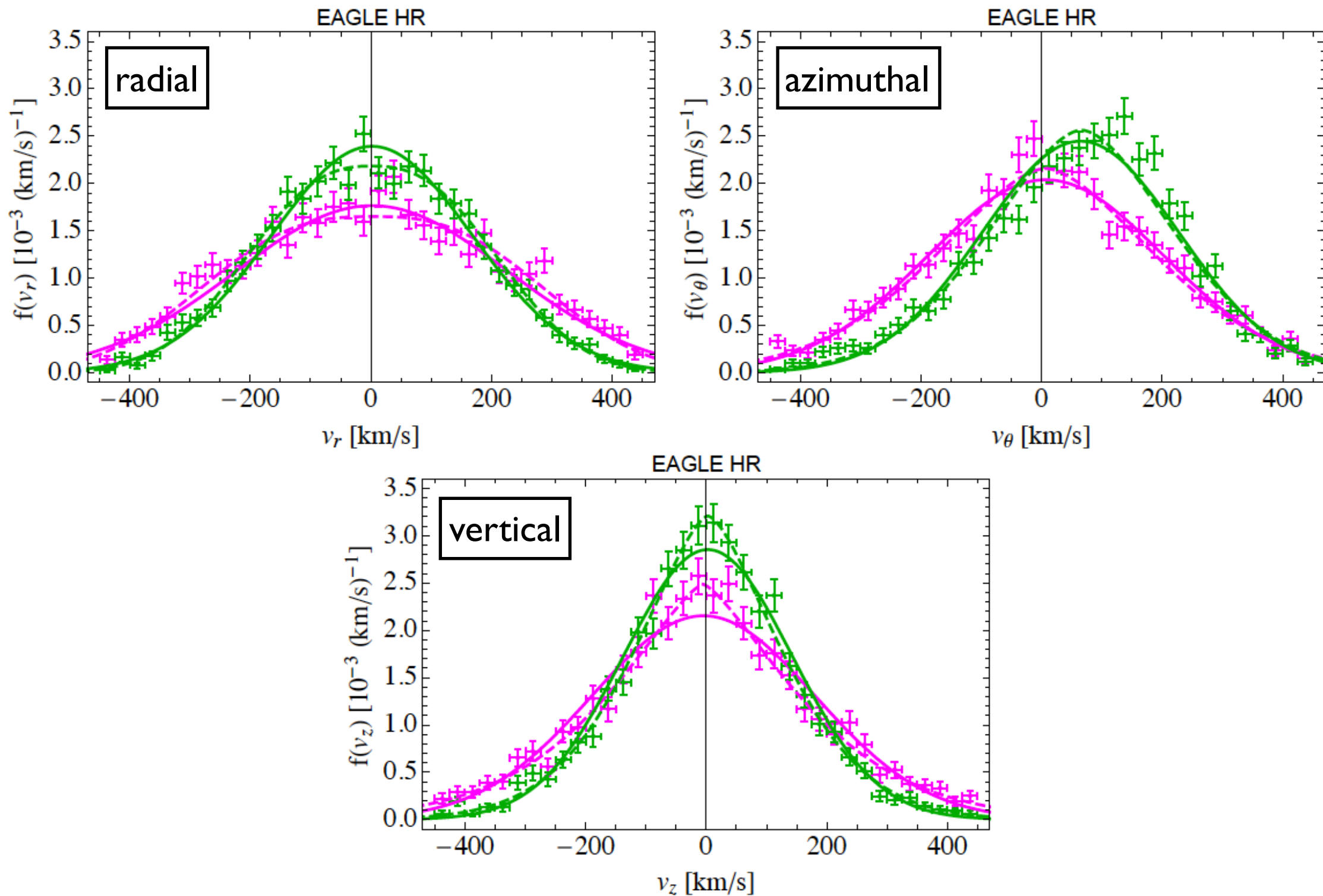
Departure from isothermal



Bozorgnia & Bertone, 1705.05853

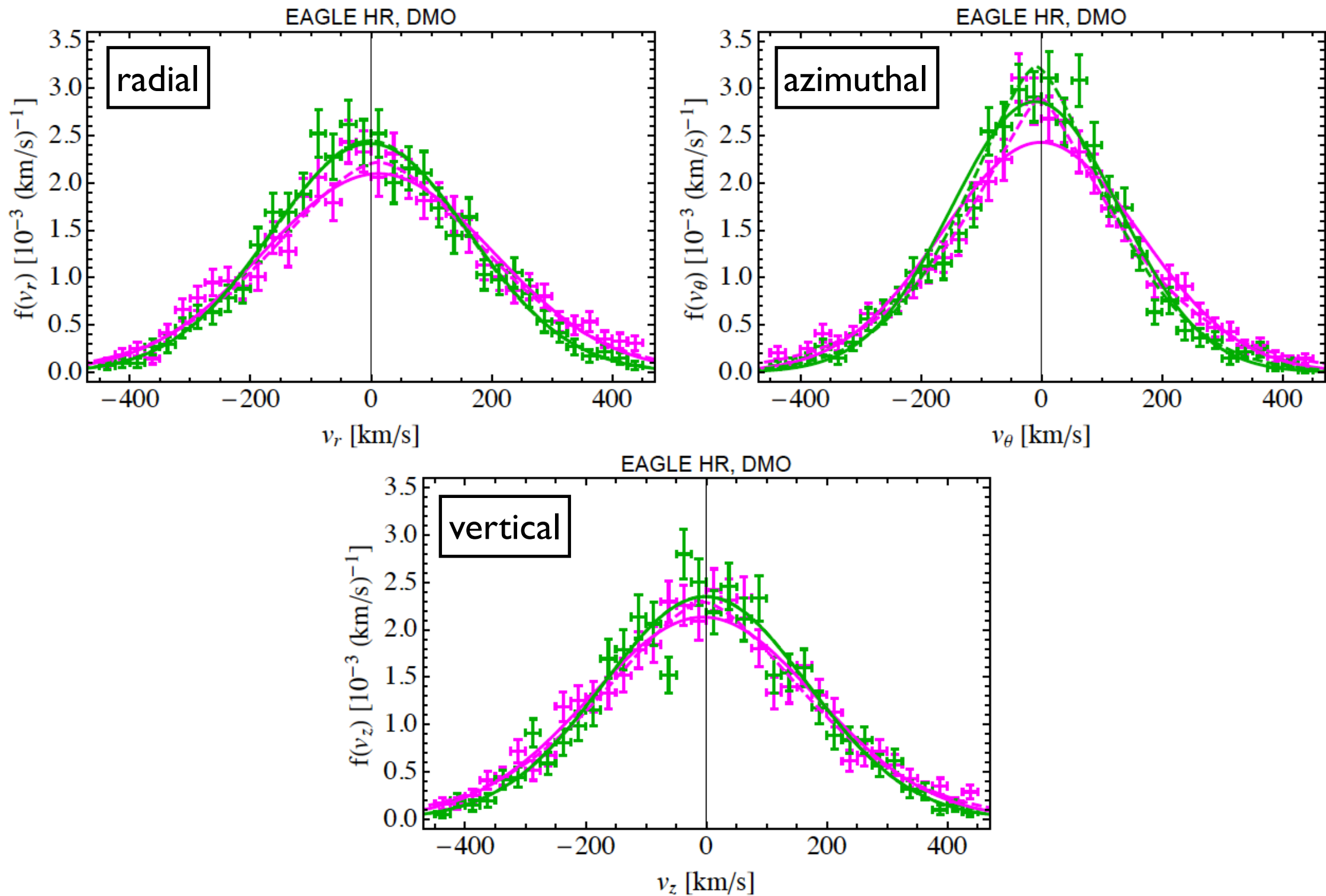
- At the Solar circle, haloes in the hydrodynamical simulation are closer to isothermal than their DMO counterparts.

Components of the velocity distribution



Bozorgnia et al., I601.04707

Comparison with DMO



Bozorgnia et al., I601.04707

How common are dark disks?

- Clear velocity anisotropy at the Solar circle.
- Two haloes have a rotating DM component in the disc with mean velocity comparable (within 50 km/s) to that of the stars.

How common are dark disks?

- Clear velocity anisotropy at the Solar circle.
- Two haloes have a rotating DM component in the disc with mean velocity comparable (within 50 km/s) to that of the stars.
- Hint for the existence of a co-rotating dark disk in 2 out of 14 MW-like haloes. → Dark disks are relatively rare in our halo sample.

Bozorgnia et al., 1601.04707

Schaller et al., 1605.02770

How common are dark disks?

- Clear velocity anisotropy at the Solar circle.
- Two haloes have a rotating DM component in the disc with mean velocity comparable (within 50 km/s) to that of the stars.
- Hint for the existence of a co-rotating dark disk in 2 out of 14 MW-like haloes. → Dark disks are relatively rare in our halo sample.

Bozorgnia et al., 1601.04707

Schaller et al., 1605.02770

- *Sizable dark disks also rare in other hydro simulations:*
 - They only appear in simulations where a large satellite merged with the MW in the recent past, which is robustly excluded from MW kinematical data.

Bozorgnia & Bertone, 1705.05853

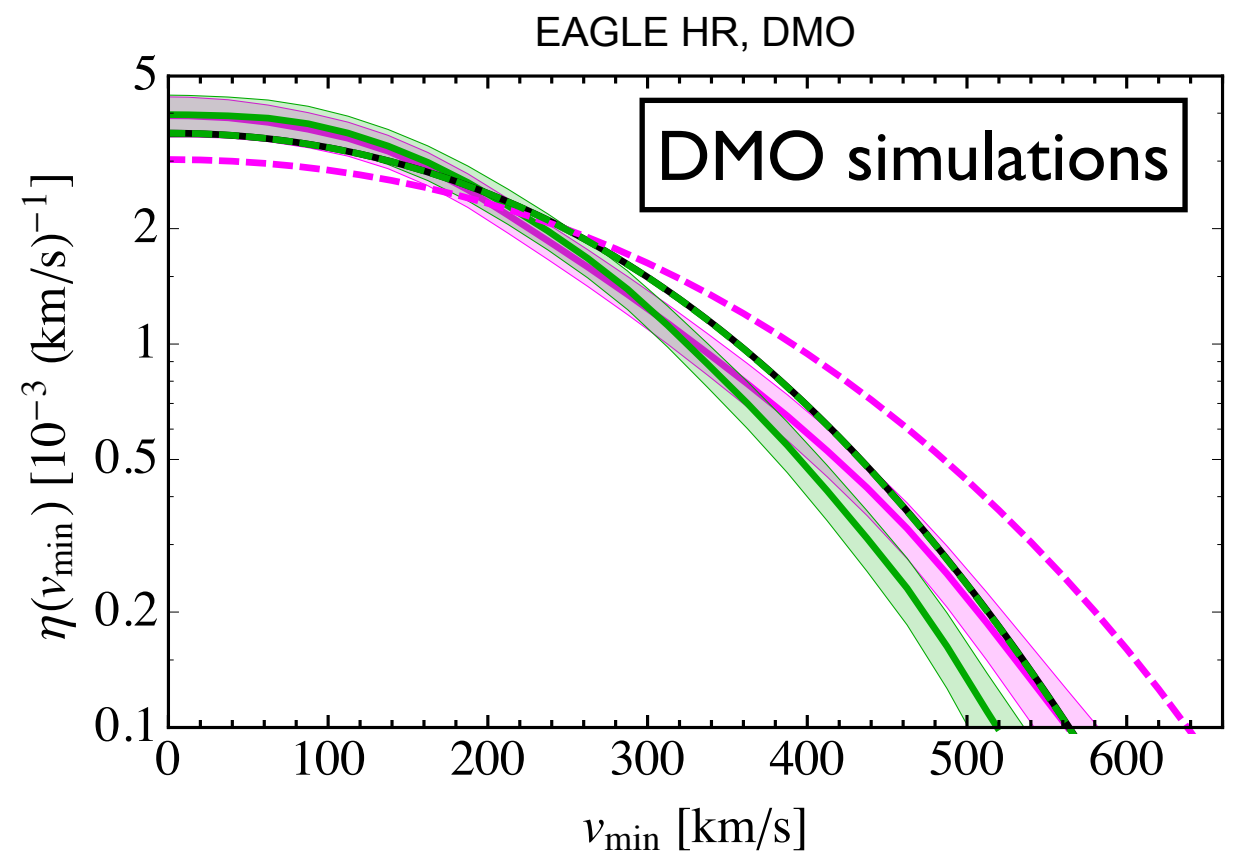
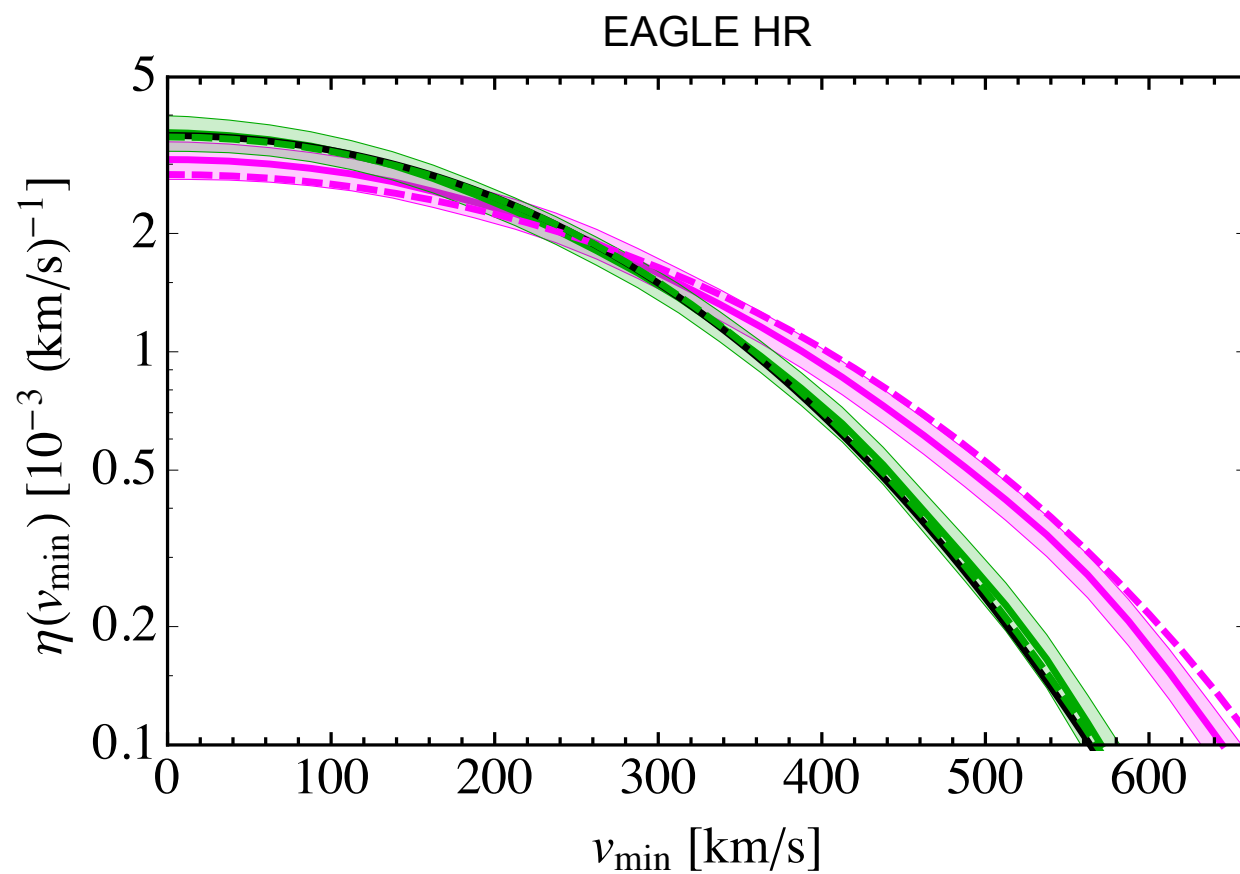
The halo integral

- For standard spin-independent and spin-dependent interactions:

$$\frac{dR}{dE_R} = \underbrace{\frac{\sigma_0 F^2(E_R)}{2m_\chi \mu_{\chi N}^2}}_{\text{particle physics}} \underbrace{\rho_\chi \eta(v_{\min}, t)}_{\text{astrophysics}}$$

$$\eta(v_{\min}, t) \equiv \int_{v > v_{\min}} d^3v \frac{f_{\text{det}}(\mathbf{v}, \mathbf{t})}{v}$$

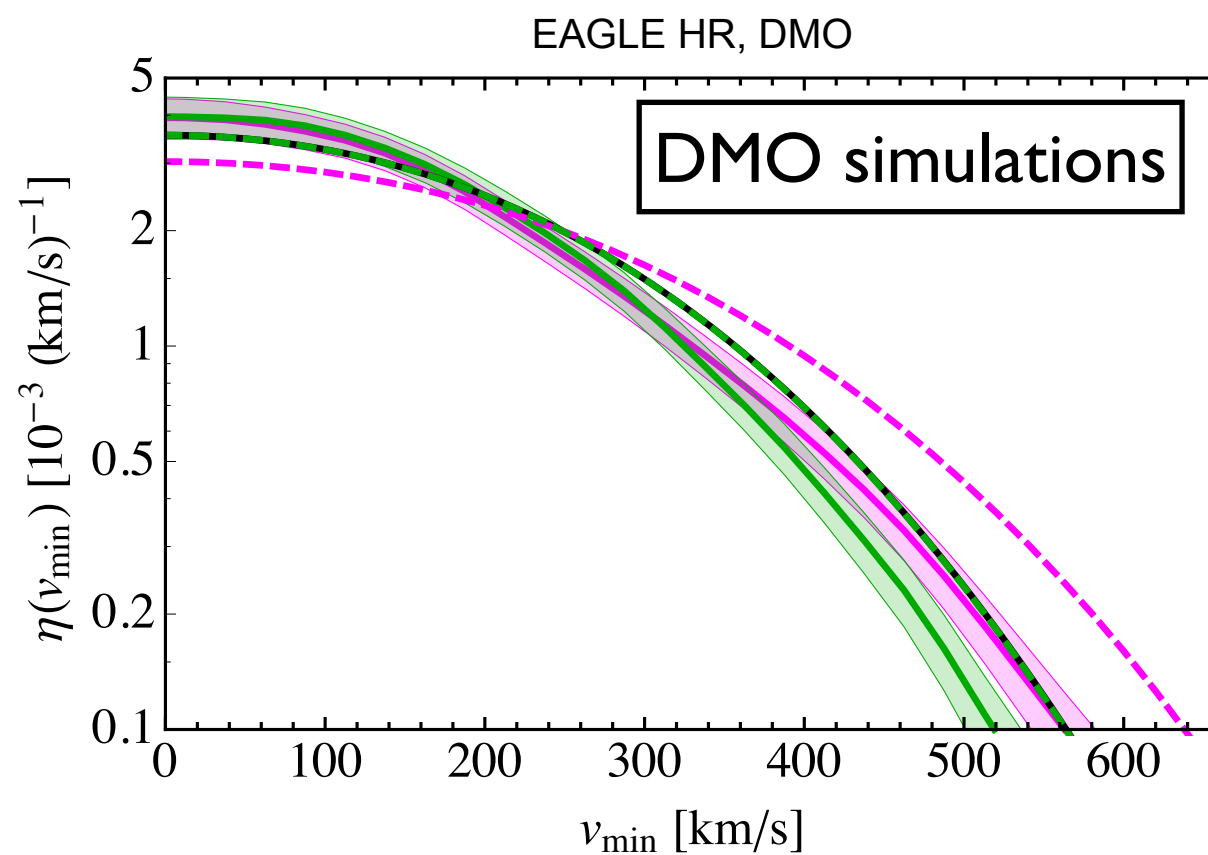
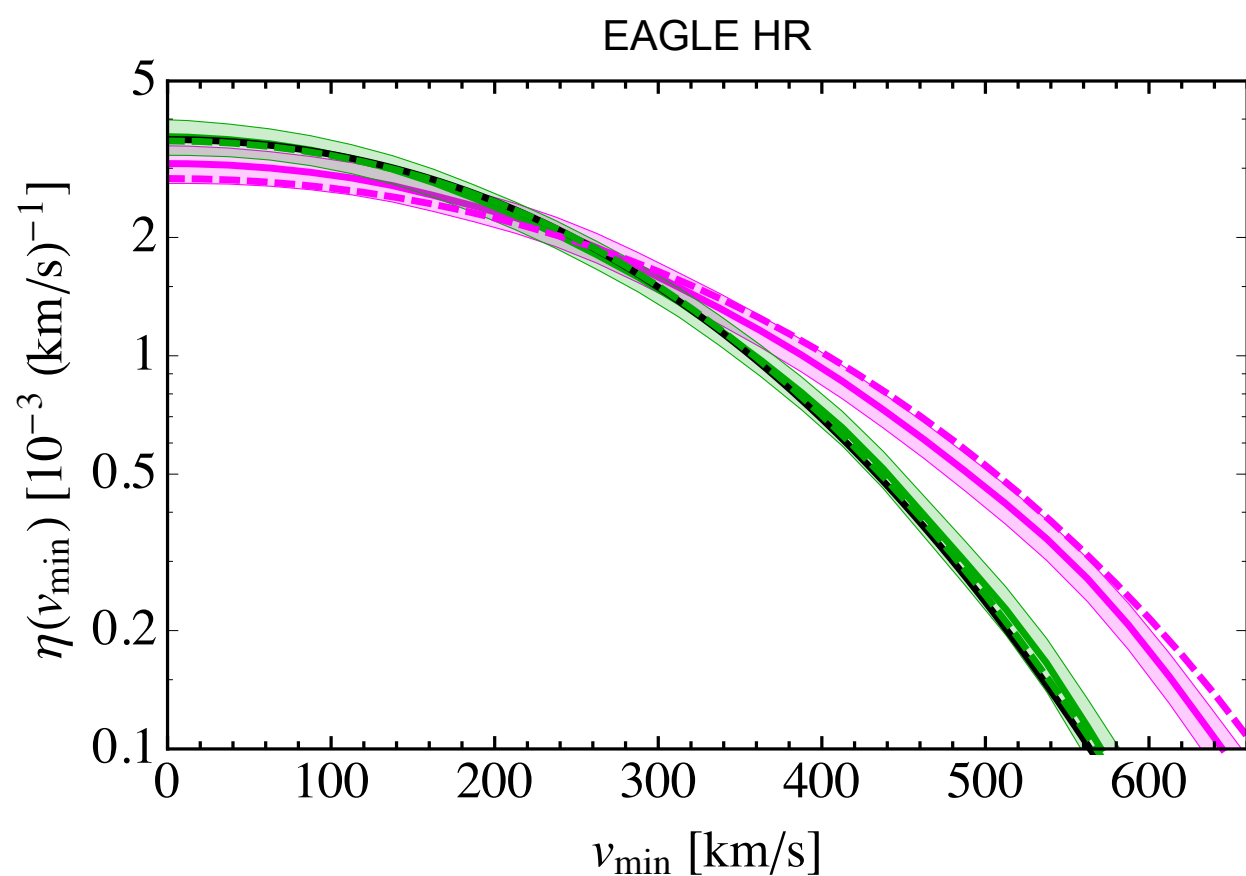
$$v_{\min} = \sqrt{m_N E_R / (2\mu_{\chi N}^2)}$$



Bozorgnia et al., 1601.04707

The halo integral

- Halo integrals for the best fit Maxwellian velocity distribution (*peak speed 223 - 289 km/s*) fall within the 1σ uncertainty band of the halo integrals of the simulated haloes.



Bozorgnia et al., 1601.04707

The halo integral

Common trend in different hydrodynamical simulations:

- Halo integrals and hence direct detection event rates obtained from a **Maxwellian velocity distribution with a free peak** are similar to those obtained directly from the simulated haloes.

Bozorgnia et al., [1601.04707](#) (EAGLE & APOSTLE)

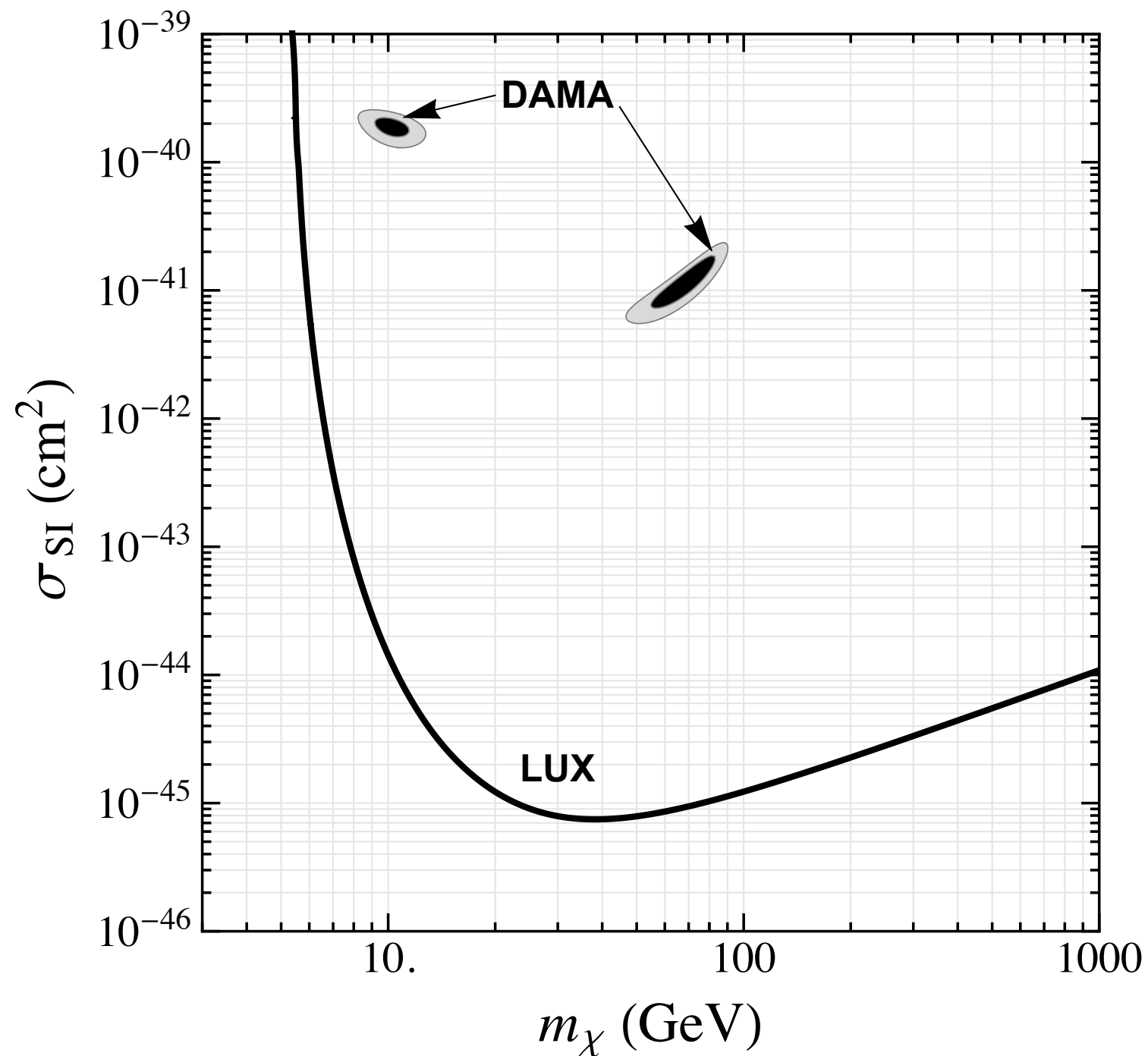
Kelso et al., [1601.04725](#) (MaGICC)

Sloane et al., [1601.05402](#)

Bozorgnia & Bertone, [1705.05853](#)

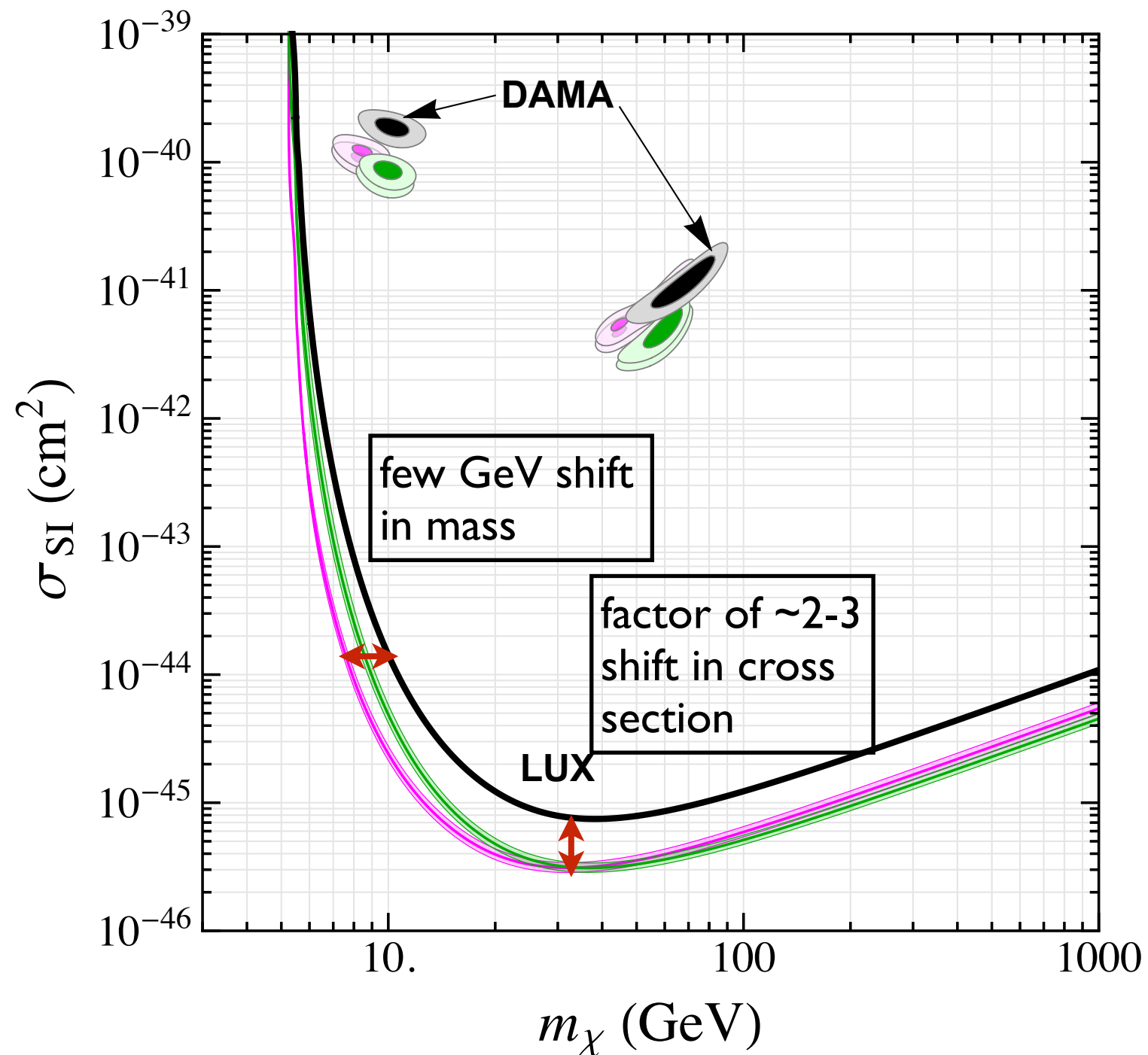
Implications for direct detection

- Assuming the **Standard Halo Model**:

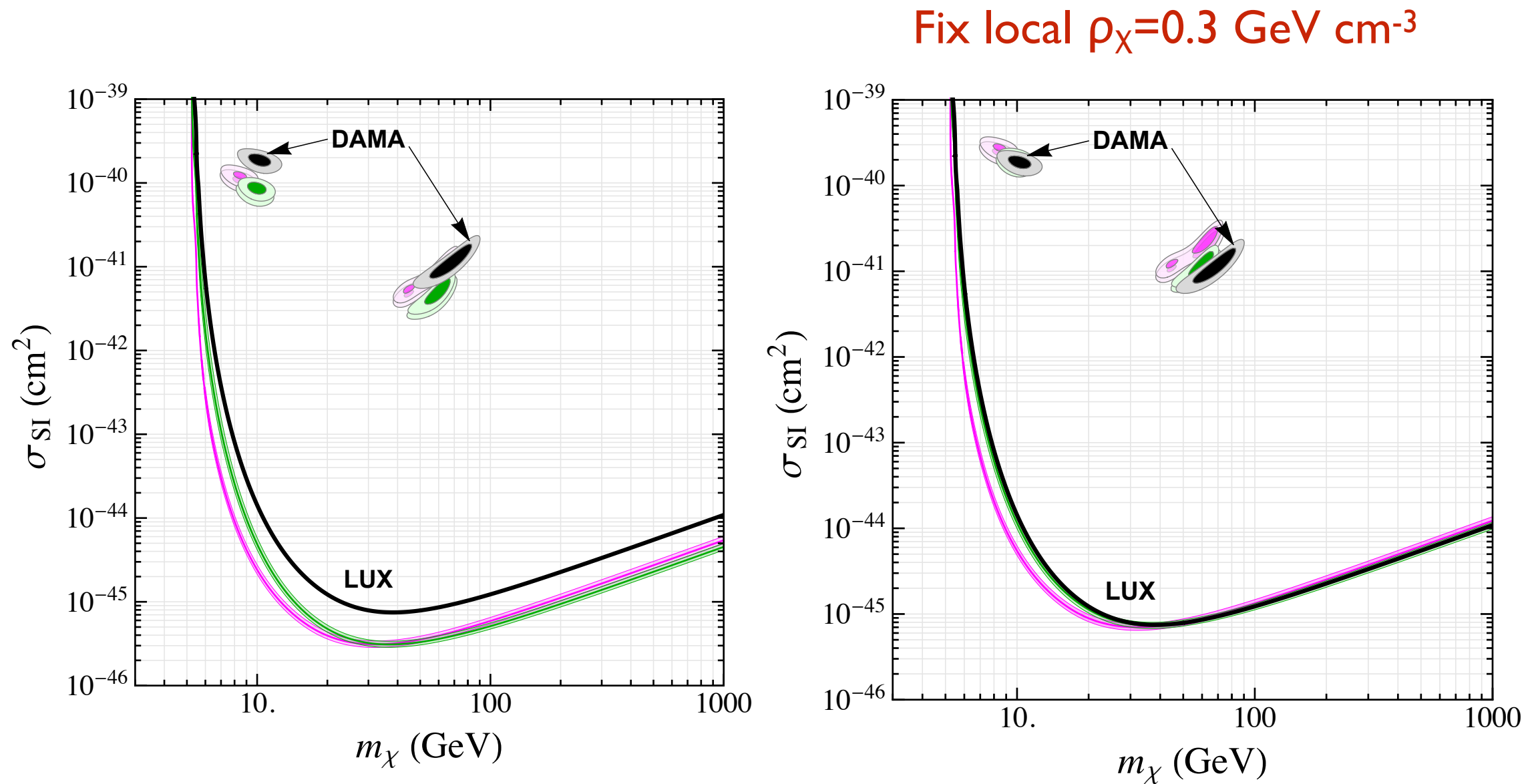


Implications for direct detection

- Compare with simulated Milky Way-like haloes:



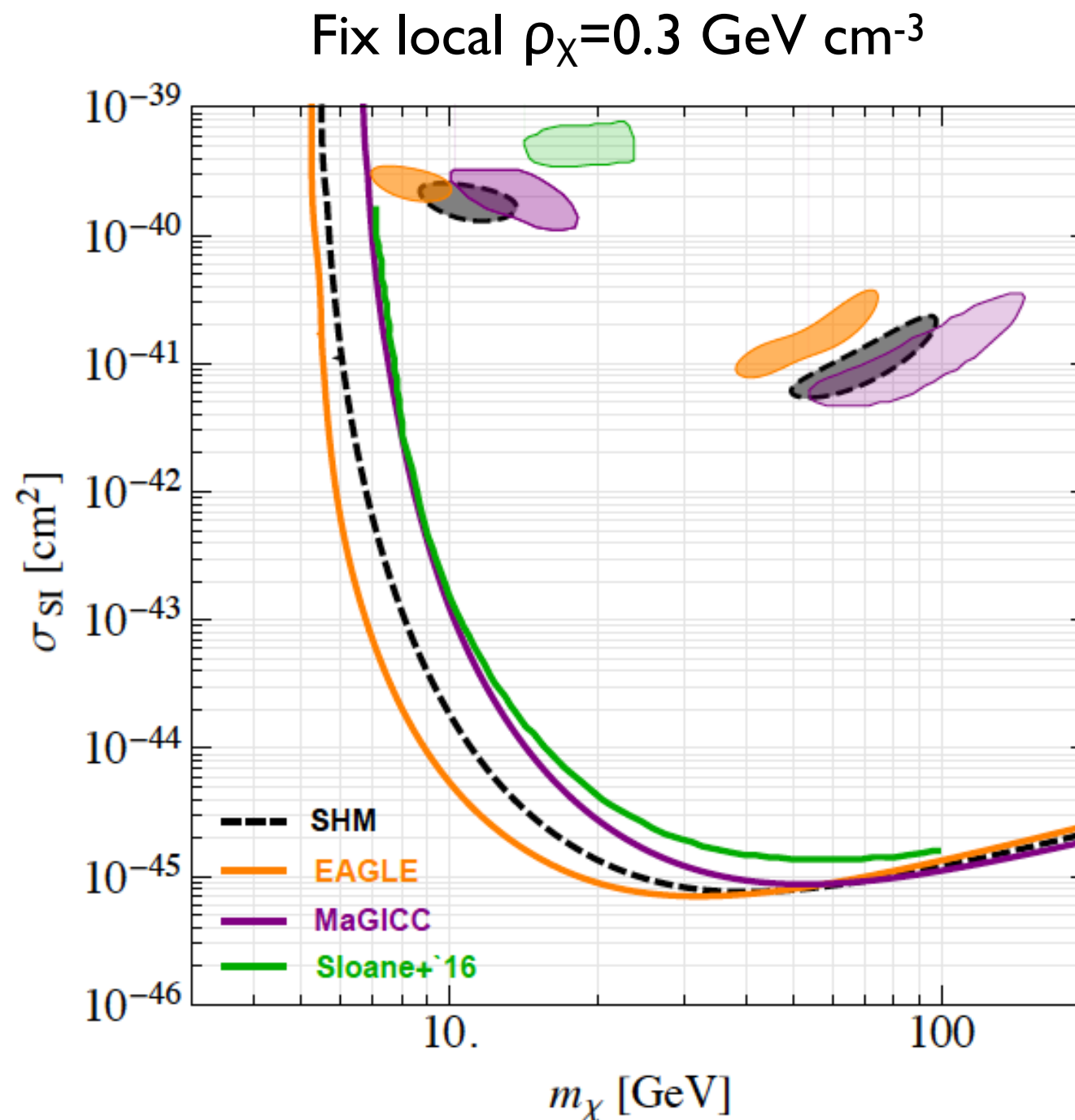
Implications for direct detection



- Difference in the local DM density \rightarrow overall difference with the SHM.
- Variation in the peak of the DM speed distribution \rightarrow shift in the low mass region.

Implications for direct detection

Comparison to other hydrodynamical simulations:



Bozorgnia & Bertone, 1705.05853

Non-standard interactions

- For a very general set of non-relativistic effective operators:

Kahlhoefer & Wild, 1607.04418

$$\frac{d\sigma_{\chi N}}{dE_R} = \frac{d\sigma_1}{dE_R} \frac{1}{v^2} + \frac{d\sigma_2}{dE_R}$$

Non-standard interactions

- For a very general set of non-relativistic effective operators:

Kahlhoefer & Wild, 1607.04418

$$\frac{d\sigma_{\chi N}}{dE_R} = \frac{d\sigma_1}{dE_R} \frac{1}{v^2} + \frac{d\sigma_2}{dE_R}$$

$\eta(v_{\min}, t)$ $h(v_{\min}, t) = \int_{v > v_{\min}} d^3v v f_{\text{det}}(\mathbf{v}, t)$

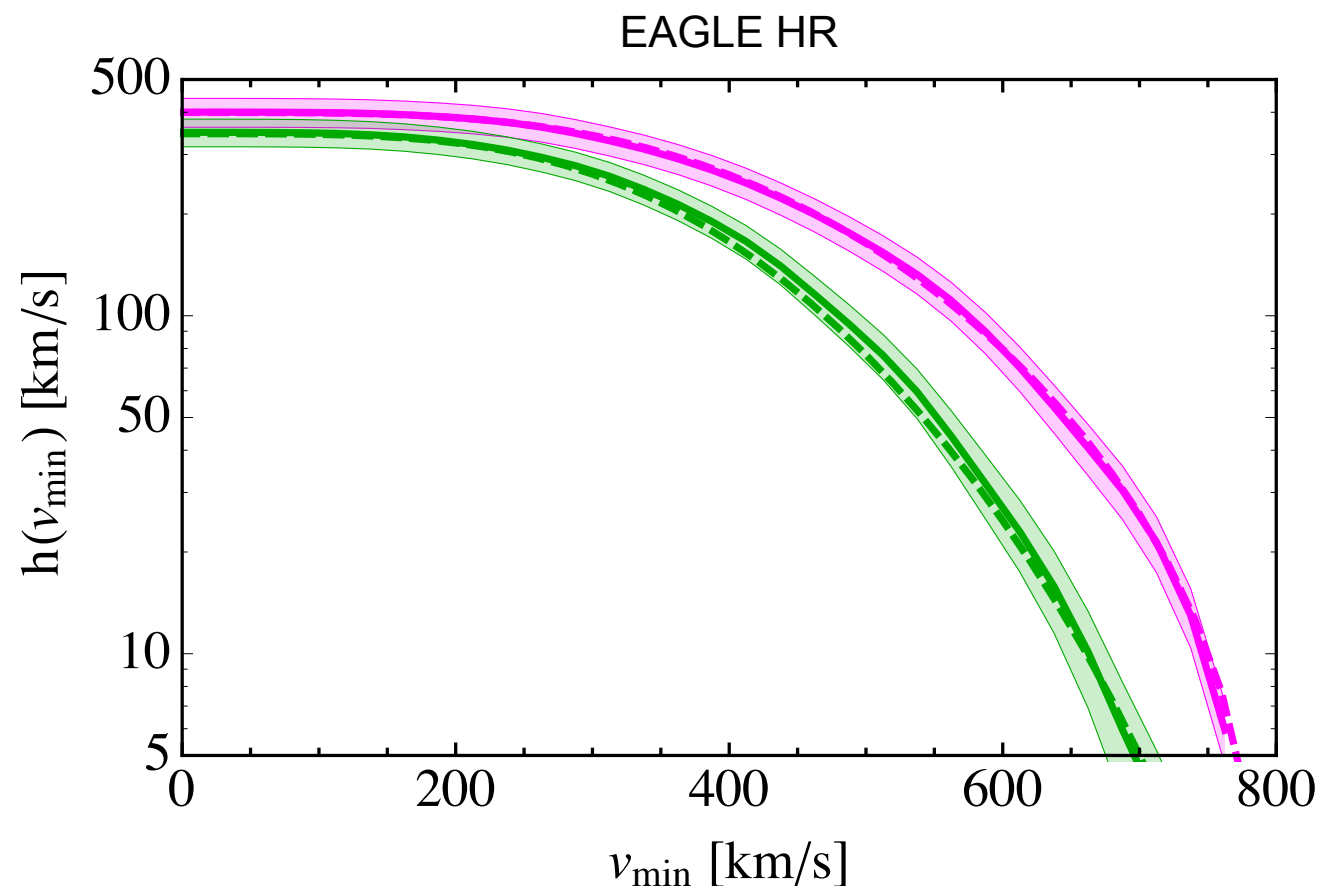
Non-standard interactions

- For a very general set of non-relativistic effective operators:

Kahlhoefer & Wild, 1607.04418

$$\frac{d\sigma_{\chi N}}{dE_R} = \underbrace{\frac{d\sigma_1}{dE_R} \frac{1}{v^2}}_{\eta(v_{\min}, t)} + \underbrace{\frac{d\sigma_2}{dE_R}}_{h(v_{\min}, t)}$$

$$h(v_{\min}, t) = \int_{v > v_{\min}} d^3v v f_{\text{det}}(\mathbf{v}, t)$$



Bozorgnia & Bertone, 1705.05853

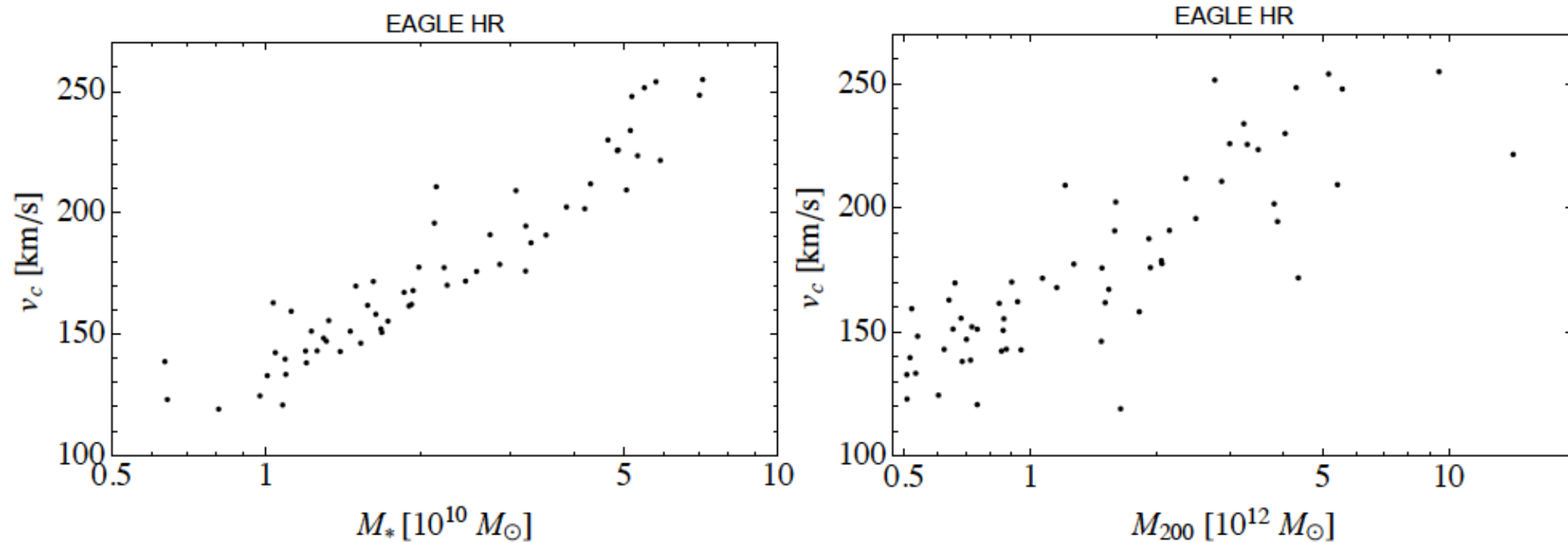
- Best fit Maxwellian $h(v_{\min})$ falls within the 1σ uncertainty band of the $h(v_{\min})$ of the simulated haloes.

Summary

- To make **precise quantitative predictions** for the DM distribution from simulations → Identify MW analogues by taking into account **observational constraints on the MW**.
- **Local DM density** agrees with local and global estimates.
Constraints from Gaia could be used in future simulations.
- **Halo integrals** of MW analogues match well those obtained from best fit Maxwellian velocity distributions.
- A **Maxwellian velocity distribution** with a **peak speed** constrained by hydrodynamical simulations could be adopted for the analysis of direct detection data. → **Can substantially reduce astrophysical uncertainties by a better selection of MW-like galaxies in simulations.**

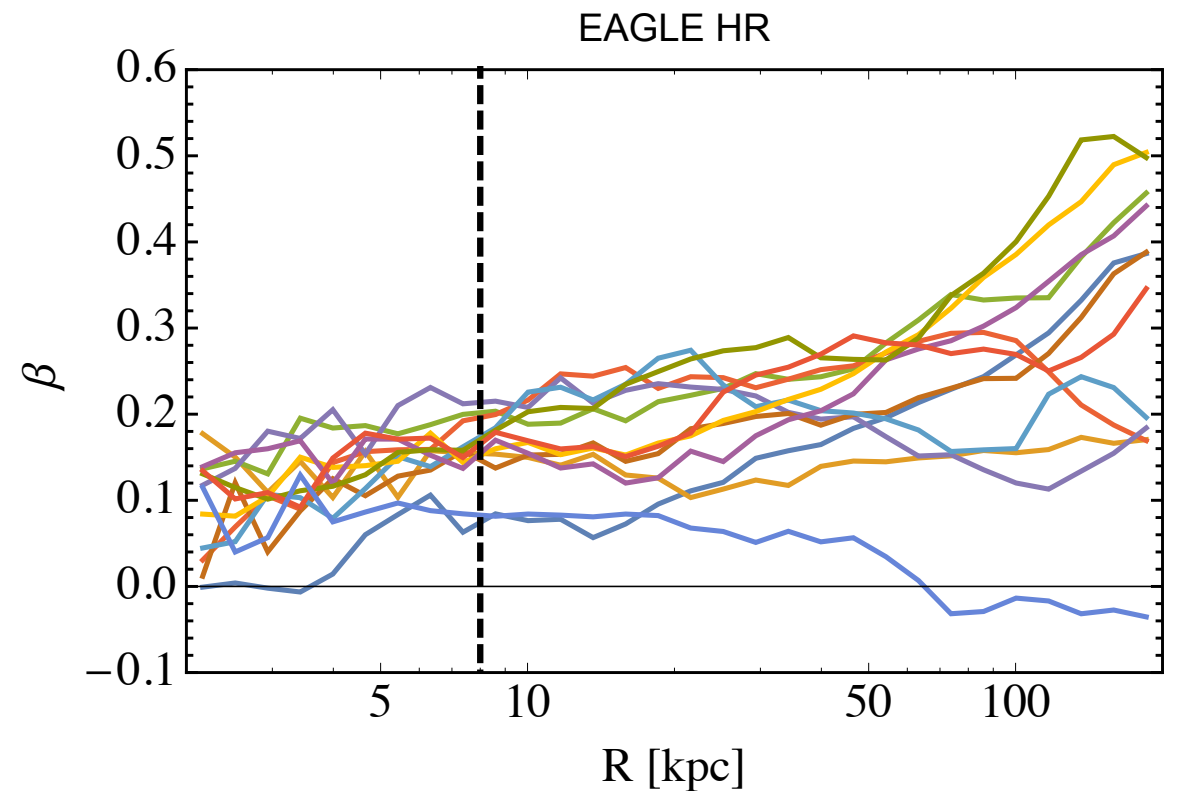
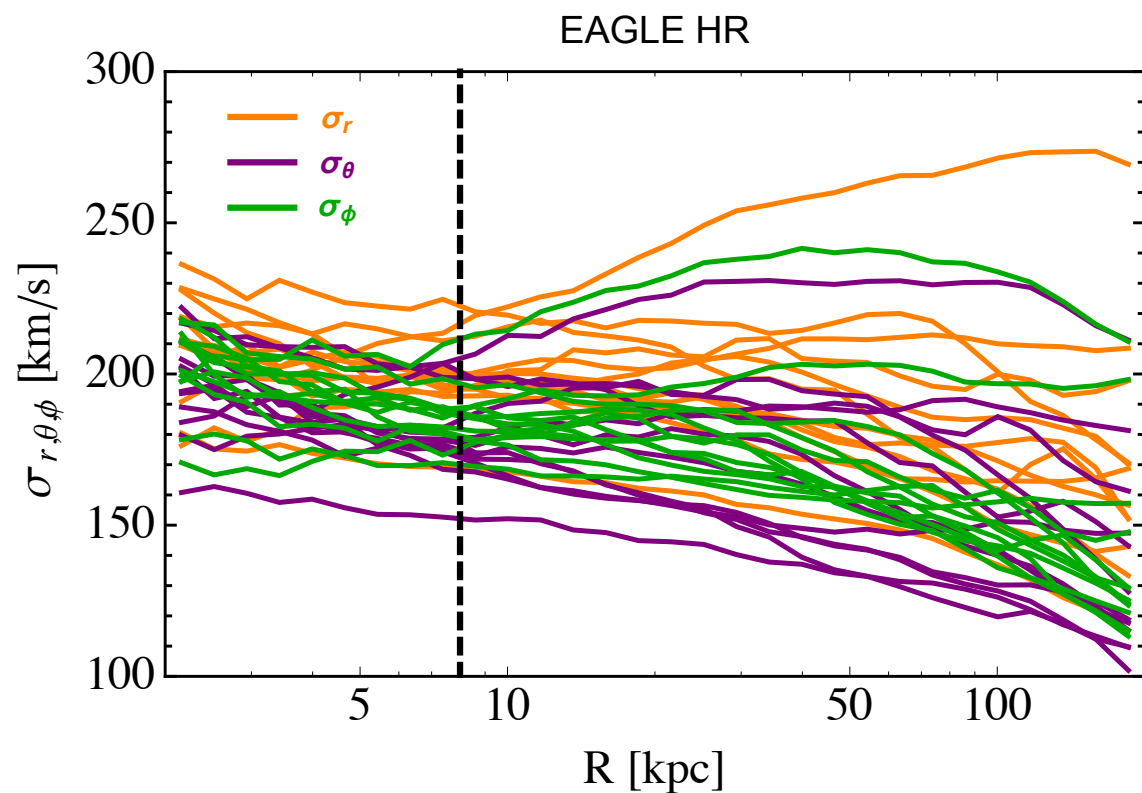
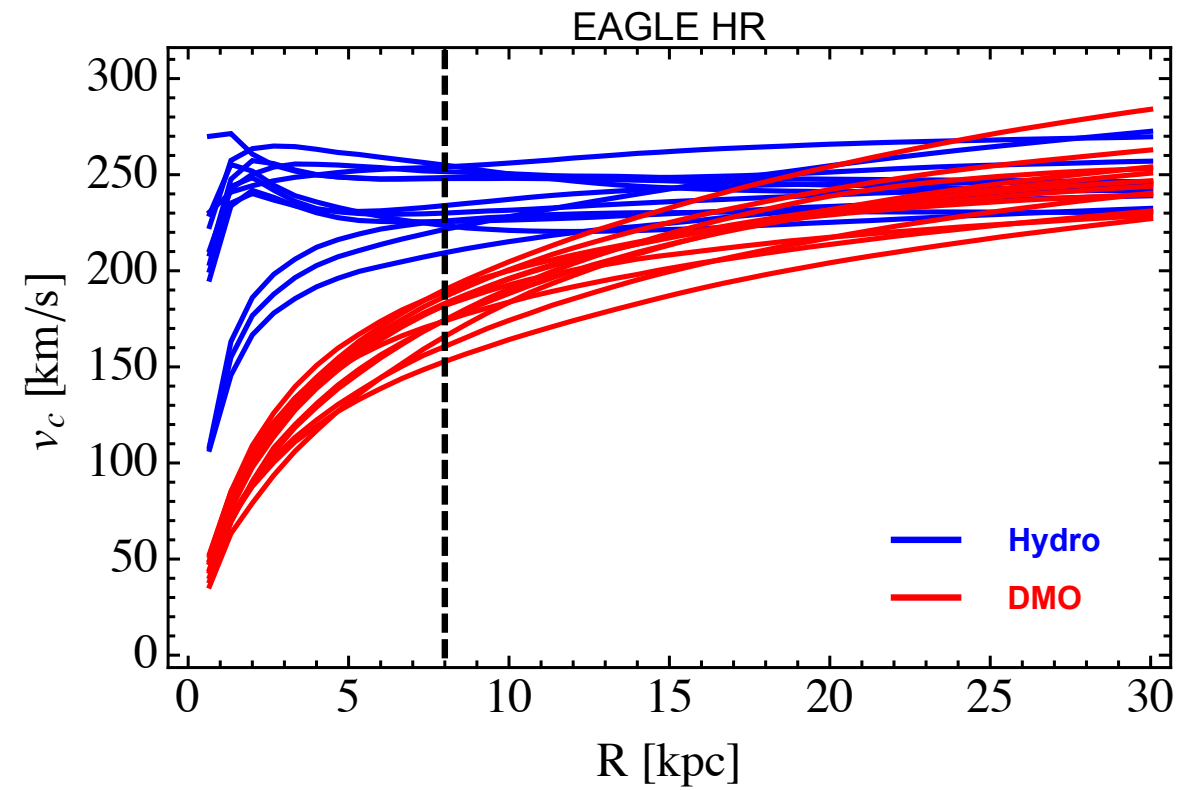
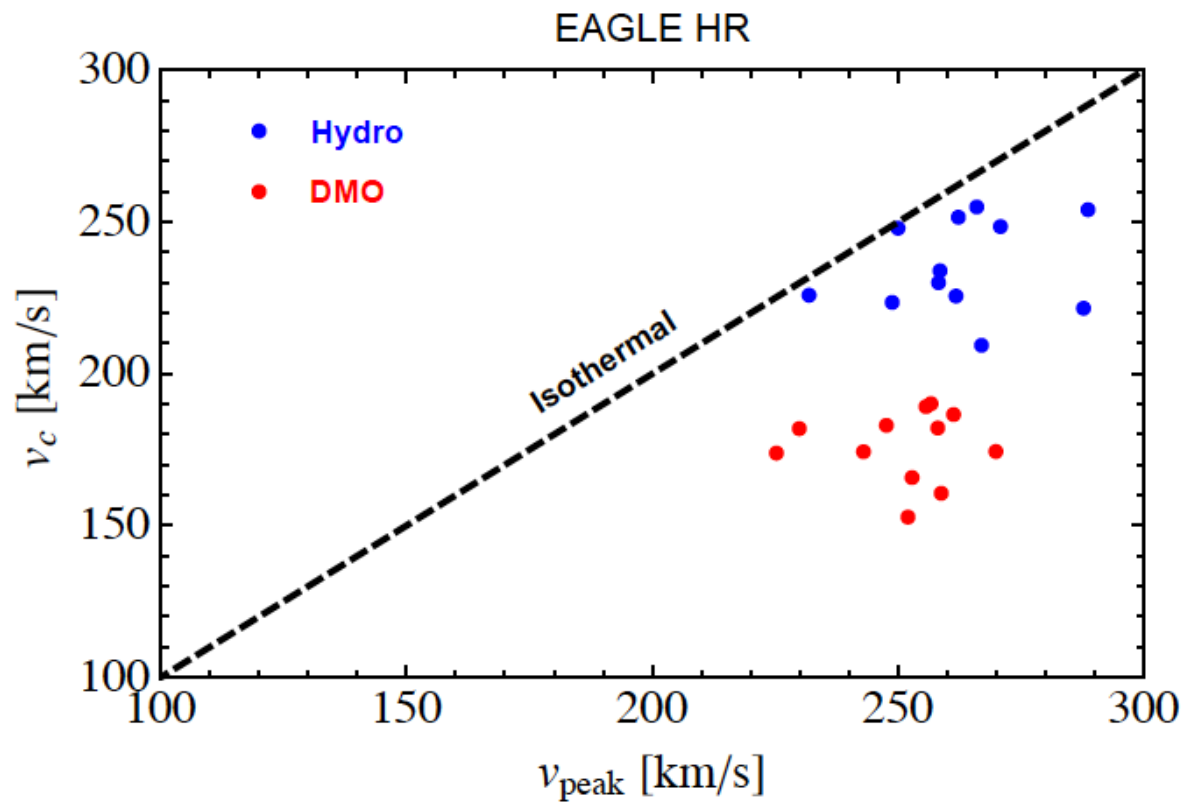
Backup Slides

Selection criteria for MW analogues



- ▶ M_* strongly correlated with v_c at 8 kpc, while the correlation of M_{200} with v_c is weaker.
- ▶ $M_*(R < 8 \text{ kpc}) = (0.5 - 0.9)M_*$.
- ▶ $M_{\text{tot}}(R < 8 \text{ kpc}) = (0.01 - 0.1)M_{200}$.
- ▶ Over the small halo mass range probed, little correlation between $M_{\text{DM}}(R < 8 \text{ kpc})$ and M_{200} .

Departure from isothermal



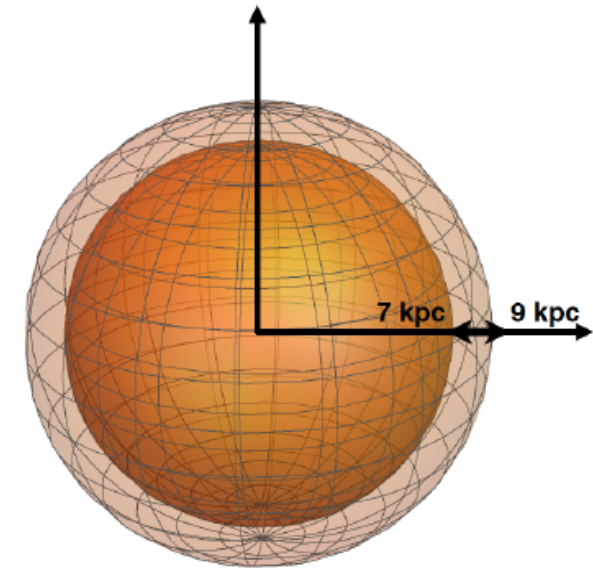
Halo shapes

Is there an enhancement of the local DM density in the **Galactic disc** compared to the **halo**?

- ▶ Compare the the average ρ_{DM} in the torus with the value in a spherical shell at $7 < R < 9$ kpc.

$\rho_{\text{DM}}^{\text{torus}}$ is larger than $\rho_{\text{DM}}^{\text{shell}}$ by:

2 – 27% for 10 haloes,
greater than 10% for 5 haloes, and
greater than 20% for only two haloes.



- ▶ The increase in the DM density in the disc could be due to the DM halo contraction as a result of dissipational baryonic processes.

Halo shapes

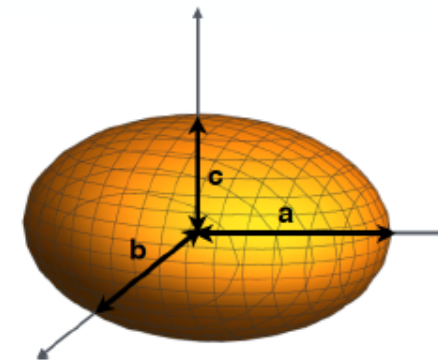
- ▶ To study the shape of the inner ($R < 8$ kpc) DM haloes, we calculate the inertia tensor of DM particles within 5 and 8 kpc.
⇒ ellipsoid with three axes of length $a \geq b \geq c$.
- ▶ Calculate the **sphericity**: $s = c/a$.
 - ▶ $s = 1$: perfect sphere. $s < 1$: increasing deviation from sphericity.
 - ▶ At 5 kpc, $s = [0.85, 0.95]$. At 8 kpc, s lower by less than 10%.
 - ▶ Due to dissipational baryonic processes, DM sphericity systematically higher in the hydrodynamic simulations compared to DMO haloes in which $s = [0.75, 0.85]$.

Halo shapes

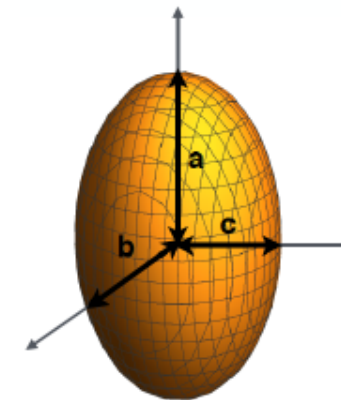
- ▶ Describe a deviation from sphericity by the triaxiality parameter:

$$T = \frac{a^2 - b^2}{a^2 - c^2}$$

- ▶ Oblate systems, $a \approx b \gg c \Rightarrow T \approx 0$.



- ▶ Prolate systems, $a \gg b \approx c \Rightarrow T \approx 1$.



- ▶ In the hydro case, since inner haloes are very close to spherical, deviation towards either oblate or prolate is small. **DMO counterparts** have a preference for *prolate* inner haloes.

Parameters of the simulations

Simulation	code	N_{DM}	$m_g [M_{\odot}]$	$m_{\text{DM}} [M_{\odot}]$	ϵ [pc]
Ling <i>et al.</i>	RAMSES	2662	–	7.46×10^5	200
Eris	GASOLINE	81213	2×10^4	9.80×10^4	124
NIHAO	EFS-GASOLINE2	–	3.16×10^5	1.74×10^6	931
EAGLE (HR)	P-GADGET (ANARCHY)	1821–3201	2.26×10^5	1.21×10^6	350
APOSTLE (IR)	P-GADGET (ANARCHY)	2160, 3024	1.3×10^5	5.9×10^5	308
MaGICC	GASOLINE	4849, 6541	2.2×10^5	1.11×10^6	310
Sloane <i>et al.</i>	GASLOINE	5847–7460	2.7×10^4	1.5×10^5	174

Properties of the selected MW analogues

Simulation	Count	$M_{\text{star}} [\times 10^{10} M_{\odot}]$	$M_{\text{halo}} [\times 10^{12} M_{\odot}]$	$\rho_{\chi} [\text{GeV}/\text{cm}^3]$	$v_{\text{peak}} [\text{km/s}]$
Ling <i>et al.</i>	1	~ 8	0.63	0.37–0.39	239
Eris	1	3.9	0.78	0.42	239
NIHAO	5	15.9	~ 1	0.42	192–363
EAGLE (HR)	12	4.65–7.12	2.76–14.26	0.42–0.73	232–289
APOSTLE (IR)	2	4.48, 4.88	1.64–2.15	0.41–0.54	223–234
MaGICC	2	2.4–8.3	0.584, 1.5	0.346, 0.493	187, 273
Sloane <i>et al.</i>	4	2.24–4.56	0.68–0.91	0.3–0.4	185–204